A variational framework for phase field modeling of elastic-plastic fracture

Brandon Talamini*[1], Michael R. Tupek[2], Andrew J. Stershic[1], and Jakob T. Ostien[1]

[1] *Sandia National Laboratories, Livermore, CA 95051, USA*
[2] *Sandia National Laboratories, Albuquerque, NM 87185, USA*

January 2020

Abstract

This paper documents a modeling framework for coupled plasticity and fracture mechanics through a phase field methodology. The distinguishing feature of this framework is that it is *variational*, in the sense that the governing equations derive from the minimization of a scalar potential. The variational approach opens the door to using robust, powerful optimization algorithms to solve the field equations. This may be particularly useful in cases where there are constraints, such as damage irreversibility and thresholds for damage initiation.

1 Introduction

Our approach follows the general framework laid out by Ortiz and Stainier (1999) and Radovitzky and Ortiz (1999). We show that an objective functional exists for which the Euler-Lagrange equations are the balance of linear momentum, the micro-force balance for the phase field, and the evolution equations for the internal variables. A consistent discretization of this functional is then formulated for numerical implementation.

2 General framework

We set down a thermodynamically consistent framework coupling rate-dependent plastic deformation and a phase field representation of fracture. We assume isotropic material behavior and isothermal conditions.

2.1 Degrees of freedom and kinematics

Let $\boldsymbol{\chi}(\boldsymbol{X}, t)$ be the deformation map at time t from the material point $\boldsymbol{X}$ in the reference configuration $B_0 \subset \mathbb{R}^3$ to the spatial point $\boldsymbol{x}$ in the current configuration $B_t \subset \mathbb{R}^3$. We denote the deformation gradient by $\boldsymbol{F} = \boldsymbol{\nabla}\boldsymbol{\chi}$, where here and in the following the operator $\boldsymbol{\nabla}$ indicates differentiation with respect to $\boldsymbol{X}$. We write $J = \det \boldsymbol{F} > 0$ for the Jacobian determinant of the deformation map. Plastic deformation is modeled through the framework of the multiplicative decomposition

$$\boldsymbol{F} = \boldsymbol{F}^e \boldsymbol{F}^p.$$

*btalami@sandia.gov

We refer to $\boldsymbol{F}^e$ and $\boldsymbol{F}^p$ as the elastic and plastic distortions. The plastic distortion $\boldsymbol{F}^p$ evolves according to the flow rule

$$\dot{\boldsymbol{F}}^p \boldsymbol{F}^{p-1} = \dot{\bar{\varepsilon}}^p \boldsymbol{N}^p, \tag{1}$$

where $\dot{\bar{\varepsilon}}^p$ is the equivalent (uniaxial) plastic strain and $\boldsymbol{N}^p$ is the flow direction. Both $\bar{\varepsilon}^p$ and $\boldsymbol{F}^p$ are taken as internal variables, which must be determined as part of the solution. Standard J_2 plasticity is adopted, hence $\boldsymbol{N}^p$ is subject to the constraints

$$\operatorname{tr} \boldsymbol{N}^p = 0, \tag{2a}$$

$$\boldsymbol{N}^p \colon \boldsymbol{N}^p = \frac{3}{2}. \tag{2b}$$

The first of these equations enforces isochoricity of plastic deformation, while the second scales $\boldsymbol{N}^p$ such that $\dot{\bar{\varepsilon}}^p$ is indeed the uniaxial effective plastic strain rate. We treat only isotropic plasticity, which permits the plastic spin to be conveniently taken as null, and therefore $\boldsymbol{N}^p$ is drawn from the space of symmetric deviatoric tensors. Plastic flow is considered irreversible in the sense

$$\dot{\bar{\varepsilon}}^p \geq 0. \tag{3}$$

Fracture is modeled with a phase field

$$\phi(\boldsymbol{X}, t), \qquad 0 \leq \phi \leq 1, \tag{4}$$

where a value of zero signifies the material at $\boldsymbol{X}$ is intact, and a value of one indicates that the material point has lost all capacity to carry load. In the models considered here, the driving force for the phase field vanishes in the limit $\phi \to 1$, and the upper bound need not be imposed as an external constraint. In contrast, the lower bound must be explicitly enforced for all of the considered models. Damage, like plastic flow, is regarded as an irreversible processes, which entails the constraint

$$\dot{\phi} \geq 0. \tag{5}$$

The collected set of kinematical degrees of freedom of the solid are

$$\{\boldsymbol{\chi}, \phi, \boldsymbol{F}^p, \bar{\varepsilon}^p\}. \tag{6}$$

2.2 Power expenditure

We use the notation

$$\mathcal{V} = \{\dot{\boldsymbol{\chi}}, \dot{\phi}, \dot{\boldsymbol{F}}^p, \dot{\bar{\varepsilon}}^p\} \tag{7}$$

to refer to the rates of change of the degrees of freedom. The expenditure of power in the body is taken to occur through the generalized velocities

$$\dot{\Lambda} = \left\{ \boldsymbol{\nabla}\dot{\boldsymbol{\chi}}, \dot{\phi}, \boldsymbol{\nabla}\dot{\phi}, \dot{\boldsymbol{F}}^p, \dot{\bar{\varepsilon}}^p \right\}. \tag{8}$$

Accordingly, we assume the existence of conjugate generalized forces

$$\mathcal{F} = \{\boldsymbol{P}, f, \boldsymbol{\xi}, \boldsymbol{T}^p, Y\}. \tag{9}$$

The power expenditure inside any part $P \subseteq B_0$ thus takes the form

$$\mathcal{P}_{\text{int}}(\mathcal{V}) = \int_P \left(\boldsymbol{P} \colon \boldsymbol{\nabla}\dot{\boldsymbol{\chi}} + \boldsymbol{T}^p \colon \dot{\boldsymbol{F}}^p + Y\dot{\bar{\varepsilon}}^p + f\dot{\phi} + \boldsymbol{\xi} \cdot \boldsymbol{\nabla}\dot{\phi} \right) \mathrm{d}V \,. \tag{10}$$

We assume external power expenditure on P has the form

$$\mathcal{P}_{\text{ext}}(\mathcal{V}) = \int_{\partial P} \boldsymbol{t}_0 \cdot \dot{\boldsymbol{\chi}} \,\mathrm{d}A + \int_B \boldsymbol{b}_0 \cdot \dot{\boldsymbol{\chi}} \,\mathrm{d}V + \int_{\partial B} \zeta_0 \dot{\phi} \,\mathrm{d}A \,, \tag{11}$$

where $\boldsymbol{t}_0$ is a surface traction (force per unit area in the reference configuration), $\boldsymbol{b}_0$ is a body force (force per unit volume in the reference configuration), and ζ_0 is a generalized surface traction that expends power through the phase-field rate. The generalized velocities $\dot{\bar{\varepsilon}}^p$ and $\dot{\boldsymbol{F}}^p$ are considered internal variables, which cannot be directly driven by external causes.

2.3 Thermodynamics

Let ψ be the free energy density (per unit volume in the reference configuration). Under isothermal conditions, the first and second laws of thermodynamics reduce to the free energy imbalance

$$\mathcal{P}_{\text{ext}}(\mathcal{V}) - \int_P \dot{\psi}\, \mathrm{d}V \geq 0.$$

From the first law of thermodynamics, we have

$$\mathcal{P}_{\text{ext}}(\mathcal{V}) = \mathcal{P}_{\text{int}}(\mathcal{V}), \tag{12}$$

so we may write

$$\mathcal{P}_{\text{int}}(\mathcal{V}) - \int_P \dot{\psi}\, \mathrm{d}V \geq 0.$$

Since this inequality must hold for any arbitrary part P, this result may be localized to yield the dissipation inequality

$$\delta = \boldsymbol{P}\colon \boldsymbol{\nabla}\dot{\boldsymbol{\chi}} + \boldsymbol{T}^p\colon \dot{\boldsymbol{F}}^p + Y\dot{\bar{\varepsilon}}^p + f\dot{\phi} + \boldsymbol{\xi}\cdot\boldsymbol{\nabla}\dot{\phi} - \dot{\psi} \geq 0. \tag{13}$$

In correspondence with the assumed form of power expenditure, the set of variables describing thermodyanamic equilibrium states is

$$\Lambda = \{\boldsymbol{F}, \phi, \boldsymbol{\nabla}\phi, \boldsymbol{F}^p, \bar{\varepsilon}^p\}\,, \tag{14}$$

and thus the constitutive relation for the free energy density must have the form

$$\psi = \psi(\boldsymbol{F}, \phi, \boldsymbol{\nabla}\phi, \boldsymbol{F}^p, \bar{\varepsilon}^p). \tag{15}$$

We allow for non-equilibrium, rate-sensitive behavior in plastic deformation and fracture. Additionally, we incorporate Newtonian viscosity, to be employed as a numerical technique to regularize snap-back. Thus, we assume that the generalized forces $\boldsymbol{P}$, Y and f may be separated additively into equilibrium and viscous (i.e., non-equilibrium) parts,

$$\begin{aligned} \boldsymbol{P} &= \boldsymbol{P}^{\text{eq}}(\Lambda) + \boldsymbol{P}^{\text{vis}}(\dot{\boldsymbol{F}}; \Lambda), \\ Y &= Y^{\text{eq}}(\Lambda) + Y^{\text{vis}}(\dot{\bar{\varepsilon}}^p; \Lambda), \\ f &= f^{\text{eq}}(\Lambda) + f^{\text{vis}}(\dot{\phi}; \Lambda). \end{aligned} \tag{16}$$

The equilibrium forces depend only on the current thermodynamic state, while the non-equilibrium forces depend on the conjugate rate variables. The non-equilibrium forces must obey

$$\begin{aligned} \lim_{\|\dot{\boldsymbol{F}}\|\to 0^+} \boldsymbol{P}^{\text{vis}} &= \boldsymbol{0}, \\ \lim_{\dot{\bar{\varepsilon}}^p \to 0^+} Y^{\text{vis}} &= 0, \\ \lim_{\dot{\phi}\to 0^+} f^{\text{vis}} &= 0, \end{aligned} \tag{17}$$

to preclude viscous dissipation in quasi-static processes. In the remaining forces $\boldsymbol{T}^p$ and $\boldsymbol{\xi}$, we do not allow for dissipative effects, and hence we write constitutive functions of the form

$$\begin{aligned} \boldsymbol{T}^p &= \boldsymbol{T}^p(\Lambda), \\ \boldsymbol{\xi} &= \boldsymbol{\xi}(\Lambda). \end{aligned} \tag{18}$$

The time derivative of the free energy function may be expanded to

$$\dot{\psi} = \frac{\partial\psi(\Lambda)}{\partial \boldsymbol{F}}\colon \dot{\boldsymbol{F}} + \frac{\partial\psi(\Lambda)}{\partial \boldsymbol{F}^p}\colon \dot{\boldsymbol{F}}^p + \frac{\partial\psi(\Lambda)}{\partial \bar{\varepsilon}^p}\dot{\bar{\varepsilon}}^p + \frac{\partial\psi(\Lambda)}{\partial \phi}\dot{\phi} + \frac{\partial\psi(\Lambda)}{\partial \boldsymbol{\nabla}\phi}\cdot\boldsymbol{\nabla}\dot{\phi}. \tag{19}$$

Inserting this identity into the dissipation inequality (13) and applying the Coleman-Noll procedure leads to several thermodynamic restrictions on the constitutive relations. The equilibrium part of the Piola stress is found to be related to the free energy through

$$\boldsymbol{P}^{\mathrm{eq}} = \frac{\partial \psi}{\partial \boldsymbol{F}}. \tag{20}$$

while the energetic resistance to plastic flow is given by

$$Y^{\mathrm{eq}} = \frac{\partial \psi}{\partial \bar{\varepsilon}^p}. \tag{21}$$

The generalized force conjugate to $\boldsymbol{F}^p$ is

$$\boldsymbol{T}^p = \frac{\partial \psi}{\partial \boldsymbol{F}^p}, \tag{22}$$

and the equilibrium part of the generalized force f is related to the free energy through

$$f^{\mathrm{eq}} = \frac{\partial \psi}{\partial \phi}. \tag{23}$$

Finally, the force conjugate to $\boldsymbol{\nabla}\dot{\phi}$ obeys the relation

$$\boldsymbol{\xi} = \frac{\partial \psi}{\partial \boldsymbol{\nabla}\phi}. \tag{24}$$

With the above restrictions, the dissipation (per unit volume in the reference configuration) is

$$\delta = \boldsymbol{P}^{\mathrm{vis}}(\dot{\boldsymbol{F}}; \Lambda) \colon \dot{\boldsymbol{F}} + f^{\mathrm{vis}}(\dot{\phi}; \Lambda)\dot{\phi} + Y^{\mathrm{vis}}(\dot{\bar{\varepsilon}}^p; \Lambda)\dot{\bar{\varepsilon}}^p. \tag{25}$$

In order to maintain a variational structure, the viscous forces are assumed to derive from dual kinetic potentials:

$$\boldsymbol{P}^{\mathrm{vis}} = \frac{\partial R^*(\dot{\boldsymbol{F}}; \Lambda)}{\partial \dot{\boldsymbol{F}}} \tag{26}$$

$$f^{\mathrm{vis}} = \frac{\partial \Phi^*(\dot{\phi}; \Lambda)}{\partial \dot{\phi}} \tag{27}$$

$$Y^{\mathrm{vis}} = \frac{\partial \Pi^*(\dot{\bar{\varepsilon}}^p; \Lambda)}{\partial \dot{\bar{\varepsilon}}^p} \tag{28}$$

In view of the restrictions (17), the (right) derivatives of the dual kinetic potentials must vanish as their arguments approach zero. For notational convenience, we collect the dual kinetic potentials into the single scalar-valued function

$$\Delta^*(\dot{\boldsymbol{F}}, \dot{\phi}, \dot{\bar{\varepsilon}}^p; \Lambda) = R^* + \Pi^* + \Phi^*. \tag{29}$$

The material is assumed to be *strictly dissipative* in the sense that

$$\begin{cases} \boldsymbol{P}^{\mathrm{vis}}(\dot{\boldsymbol{F}}; \Lambda) \colon \dot{\boldsymbol{F}} > 0, & \text{if } \dot{\boldsymbol{F}} \neq \boldsymbol{0}; \\ f^{\mathrm{vis}}(\dot{\phi}; \Lambda)\, \dot{\phi} > 0, & \text{if } \dot{\phi} \neq 0. \\ Y^{\mathrm{vis}}(\dot{\bar{\varepsilon}}^p; \Lambda)\, \dot{\bar{\varepsilon}}^p > 0, & \text{if } \dot{\bar{\varepsilon}}^p \neq 0; \end{cases} \tag{30}$$

Satisfaction of the dissipation inequality is then ensured if each dual kinetic potential obeys the following conditions:[1]

(C1) the dual kinetic potential is convex in its rate variable (for every Λ);

(C2) the dual kinetic potential achieves its minimum (for every Λ) when the rate variable is zero.

In specifying the constitutive relations, we shall confine ourselves to dual kinetic potentials with properties (C1) and (C2), so that compliance with the dissipation inequality is guaranteed.

[1] This may be demonstrated as follows. Convexity of Π^* means that

$$\Pi^*(\widetilde{\dot{\bar{\varepsilon}}}^p) \geq \Pi^*(\dot{\bar{\varepsilon}}^p) + \frac{\partial \Pi^*(\dot{\bar{\varepsilon}}^p)}{\partial \dot{\bar{\varepsilon}}^p}(\widetilde{\dot{\bar{\varepsilon}}}^p - \dot{\bar{\varepsilon}}^p),$$

3 Specialization of constitutive relations

The free energy is assumed to decompose additively into an elastic contribution, a plastic contribution representing the stored energy of cold work[2], and a contribution due to fracture:

$$\psi = \psi^e(\boldsymbol{F}, \boldsymbol{F}^p, \phi) + \psi^p(\bar{\varepsilon}^p, \phi) + \psi^f(\phi, \boldsymbol{\nabla}\phi). \tag{31}$$

In the following section, we specify first the free energy and kinetic equations prescribing the mechanical elastic-plastic behavior of the solid. The fracture constitutive relations are taken up in Section 3.2.

3.1 Mechanical constitutive relations

Following the standard phase field fracture modeling approach, the elastic free energy density is taken to be the product of an energy density $\tilde{\psi}^e$ which represents the behavior of the material in the absence of damage, and a degradation function $g(\phi)$, representing the gradual loss of integrity due to damage:

$$\psi^e(\boldsymbol{F}, \boldsymbol{F}^p, \phi) = g(\phi)\widetilde{\psi}^e(\boldsymbol{F}^e), \tag{32}$$

This framework, wherein a constitutive function for the intact material is multiplied by a degradation function, is re-used in several points. We adopt the convention that a quantity under a tilde $\widetilde{\bullet}$ represents a constitutive function for the *intact* material, by which we mean in the absence of damage. Regarding $g(\phi)$, one aim of this paper is to compare different functional forms, so we leave the it unspecified for the moment. It suffices to say at this point that it is a monotonically decreasing function that satisfies the conditions

$$g(0) = 1, \quad g(1) = 0, \tag{33}$$

so that the elastic energy storage capacity decreases as damage increases, and all load carrying capacity is lost as $\phi \to 1$. We discuss particular choices of the degradation functions in Section 3.4.

Note that the free energy depends on $\boldsymbol{F}$ and $\boldsymbol{F}^p$ solely through the elastic distortion tensor $\boldsymbol{F}^e = \boldsymbol{F}\boldsymbol{F}^{p-1}$. Frame indifference further demands that the constitutive function for the elastic free energy depend on $\boldsymbol{F}^e$ through $\boldsymbol{C}^e = \boldsymbol{F}^{eT}\boldsymbol{F}^e$. For the intact elastic free energy, we choose the isotropic Hencky elasticity model:

$$\widetilde{\psi}^e = \mu\|\mathrm{dev}(\boldsymbol{\varepsilon}^e)\|^2 + \frac{\kappa}{2}\,\mathrm{tr}^2(\boldsymbol{\varepsilon}^e), \tag{34}$$

where $\boldsymbol{\varepsilon}^e = \frac{1}{2}\log(\boldsymbol{C}^e)$ is the logarithmic elastic strain tensor.

The dual kinetic potential for the viscous stress is taken to be

$$R^*(\dot{\boldsymbol{F}}; \boldsymbol{F}, \phi) = g(\phi)\widetilde{R}^*(\dot{\boldsymbol{F}}; \boldsymbol{F}), \tag{35}$$

where the intact part is

$$\widetilde{R}^*(\dot{\boldsymbol{F}}; \boldsymbol{F}) = J\eta\|\mathrm{dev}(\boldsymbol{D})\|^2, \quad \boldsymbol{D} = \mathrm{sym}\left(\dot{\boldsymbol{F}}\boldsymbol{F}^{-1}\right), \tag{36}$$

which is the Rayleigh dissipation function for Newtonian viscous stress. The parameter η is the viscosity.

The stored energy of cold work is also taken to be the product of a degradation function and an intact response function:

$$\psi^p(\bar{\varepsilon}^p, \phi) = g^p(\phi)\widetilde{\psi}^p(\bar{\varepsilon}^p). \tag{37}$$

---

for all nonnegative $\widetilde{\bar{\varepsilon}}^p$ and $\dot{\bar{\varepsilon}}^p$. Let us take $\widetilde{\bar{\varepsilon}}^p = 0$. Then by (C2), Π^* reaches the minimum value at $\widetilde{\bar{\varepsilon}}^p$, call it $\Pi^*_{\min}$, and we have

$$\frac{\partial\Pi^*(\dot{\bar{\varepsilon}}^p)}{\partial\dot{\bar{\varepsilon}}^p}\dot{\bar{\varepsilon}}^p \geq \Pi^*(\dot{\bar{\varepsilon}}^p) - \Pi^*_{\min}$$

or

$$Y^{\mathrm{vis}}\dot{\bar{\varepsilon}}^p \geq \Pi^*(\dot{\bar{\varepsilon}}^p) - \Pi^*_{\min} \geq 0.$$

Identical proofs hold for $R^*(\dot{\boldsymbol{F}}; \Lambda)$ and $\Delta^*(\dot{\phi}; \Lambda)$.

[2] Kinematic hardening could be included in ψ^p through an explicit dependence on $\boldsymbol{F}^p$, but we examine only monotonic loading problems in this paper, which do not benefit from this additional complication.

Note the degradation function $g^p(\phi)$ is not necessarily identical to $g(\phi)$; as with the elastic degradation function, we discuss particular choices in Section 3.4. Any well-behaved hardening law can be chosen for $\widetilde{\psi}^p(\bar{\varepsilon}^p)$. In a similar vein, the dual kinetic potential for the over-stress is taken as

$$\Pi^*(\dot{\bar{\varepsilon}}^p;\phi) = g^p(\phi)\widetilde{\Pi}^*(\dot{\bar{\varepsilon}}^p), \tag{38}$$

where $\widetilde{\Pi}^*(\dot{\bar{\varepsilon}}^p)$ is a dual kinetic potential describing the rate sensitivity of the intact material.

Remark 3.1. The framework is quite flexible in the choice of stored cold work and rate sensitivity. For example, a form of power law hardening can be obtained by taking

$$\widetilde{\psi}^p(\bar{\varepsilon}^p) = \frac{n\sigma_y\epsilon_0}{(n+1)}\left[\left(1+\frac{\bar{\varepsilon}^p}{\epsilon_0}\right)^{\frac{1+n}{n}} - 1\right], \tag{39}$$

where the parameters of the model are n, the hardening index, σ_y, the yield strength, and ϵ_0, a reference strain value.[3] The equilibrium flow strength follows from Eq. (21) as

$$Y^{\rm eq} = g^p(\phi)\sigma_y\left(1+\frac{\bar{\varepsilon}^p}{\epsilon_0}\right)^{1/n}. \tag{40}$$

Classic power law rate sensitivity is obtained by taking

$$\widetilde{\Pi}^*(\dot{\bar{\varepsilon}}^p) = \begin{cases} \infty, & \dot{\bar{\varepsilon}}^p < 0 \\ \frac{m\sigma_y\dot{\epsilon}_0}{m+1}\left(\frac{\dot{\bar{\varepsilon}}^p}{\dot{\epsilon}_0}\right)^{(1+m)/m}, & \dot{\bar{\varepsilon}}^p \geq 0 \end{cases} \tag{41}$$

with m the rate sensitivity exponent and $\dot{\epsilon}_0$ a reference strain rate value. Using Eq. (28) the viscous over-stress is then

$$Y^{\rm vis} = g^p(\phi)\sigma_y\left(\frac{\dot{\bar{\varepsilon}}^p}{\dot{\epsilon}_0}\right)^{1/m}, \tag{42}$$

whenever $\dot{\bar{\varepsilon}}^p \geq 0$. Many other commonly used hardening laws and rate sensititivity laws can be cast in variational form; for more examples, see Ortiz and Stainier (1999). □

3.2 Fracture constitutive relations

A conventional form is adopted for the fracture energy

$$\psi^f(\phi,\boldsymbol{\nabla}\phi) = \frac{3G_c}{8\ell}\left(\phi + \ell^2\|\boldsymbol{\nabla}\phi\|^2\right) \tag{43}$$

see, for example Pham et al. (2011). Regarding Eq. (43), G_c represents the critical energy release rate (or in view of the elastic-plastic behavior, the initiation energy release rate) in terms of energy per unit area in the reference configuration, and ℓ is the regularization length scale. The particular form of the fracture energy prescribed by (43) introduces a threshold for phase (damage) to nucleate; see Pham et al. (2011).

The dual kinetic potential for the phase rate is taken to be the simple quadratic form

$$\Phi^*(\dot{\phi}) = \frac{\beta\dot{\phi}^2}{2}, \tag{44}$$

where $\beta \geq 0$ is the kinetic modulus. We leave open the possibility for quasi-static phase field evolution in which case this this potential term is omitted; alternatively, one may regard the quasi-static case as the limit of $\beta \to 0$.

[3] Note that the constant term in the power law cannot be dropped. The function $\widetilde{\psi}^p$ enters the free energy as a factor multiplying the degradation function, and hence dropping the constant term leads to a shift in the free energy not by a constant, but by a function of the phase field. This is ia notable departure from conventional plasticity theory that must be ensured if re-using code. Thanks to Gary Hu for pointing this out.

3.3 Auxiliary constitutive equations

With the functional forms of the free energy and the dual kinetic potentials specified, explicit forms of the generalized forces can be determined. Applying the thermodynamic identity (20) gives

$$\begin{aligned}\boldsymbol{P}^{\mathrm{eq}} &= \frac{\partial \psi(\Lambda)}{\partial \boldsymbol{F}} \\ &= \frac{\partial \psi^e(\boldsymbol{F}^e, \phi)}{\partial \boldsymbol{F}^e} : \frac{\partial \boldsymbol{F}^e}{\partial \boldsymbol{F}} \\ &= \boldsymbol{T}^e \boldsymbol{F}^{p-T},\end{aligned} \tag{45}$$

where we have defined $\boldsymbol{T}^e = \partial \psi^e / \partial \boldsymbol{F}^e$. This in turn can be used to relate the stress $\boldsymbol{T}^p$ to the Piola stress. Indeed,

$$\begin{aligned}\boldsymbol{T}^p &= \frac{\partial \psi(\Lambda)}{\partial \boldsymbol{F}^p} \\ &= \frac{\partial \psi^e(\boldsymbol{F}^e, \phi)}{\partial \boldsymbol{F}^e} : \frac{\partial \boldsymbol{F}^e}{\partial \boldsymbol{F}^p} \\ &= -\boldsymbol{F}^{eT} \boldsymbol{T}^e \boldsymbol{F}^{p-T},\end{aligned}$$

which, upon comparison with (45) yields

$$\boldsymbol{T}^p = -\boldsymbol{F}^{eT} \boldsymbol{P}^{\mathrm{eq}}. \tag{46}$$

Writing $\boldsymbol{\Sigma}$ for the stress conjugate to the logarithmic elastic strains $\boldsymbol{\varepsilon}^e$, we have

$$\boldsymbol{\Sigma} = \frac{\partial \psi}{\partial \boldsymbol{\varepsilon}^e} = g(\phi) \left[2\mu \operatorname{dev}(\boldsymbol{\varepsilon}^e) + \kappa \operatorname{tr}(\boldsymbol{\varepsilon}^e) \mathbf{1} \right] \tag{47}$$

It will be convenient to introduce the Mandel stress

$$\boldsymbol{M} = -\boldsymbol{T}^p \boldsymbol{F}^{pT} = \boldsymbol{F}^{eT} \boldsymbol{P}^{\mathrm{eq}} \boldsymbol{F}^{pT}. \tag{48}$$

It can be shown that for isotropic materials, the Mandel stress and $\boldsymbol{\Sigma}$ coincide.[4] This is convenient, as the Mandel stress then appears both in the yield function and in the elastic relation in a role that is analogous to the stress tensor in small-strain plasticity theory (cf. 67). Given this coincidence, we can write

$$\boldsymbol{M} = g(\phi) \left[2\mu \operatorname{dev}(\boldsymbol{\varepsilon}^e) + \kappa \operatorname{tr}(\boldsymbol{\varepsilon}^e) \mathbf{1} \right] \tag{49}$$

and the equilibrium part of the Piola stress as

$$\boldsymbol{P}^{\mathrm{eq}} = \boldsymbol{F}^{e-T} \boldsymbol{M} \boldsymbol{F}^{p-T}. \tag{50}$$

The viscous part of the Piola stress follows from (26), (35), and (36) as

$$\boldsymbol{P}^{\mathrm{vis}} = g(\phi) J \widetilde{\boldsymbol{T}}^{\mathrm{vis}} \boldsymbol{F}^{-T}, \quad \widetilde{\boldsymbol{T}}^{\mathrm{vis}} = 2\eta \operatorname{dev} \boldsymbol{D}. \tag{51}$$

From (23) and (26), the generalized forces associated with the phase field are found to be

$$\begin{aligned} f^{\mathrm{eq}} &= \frac{3G_c}{8\ell} + g'(\phi) \widetilde{\psi}^e + g^{p\prime}(\phi) \widetilde{\psi}^p, \\ f^{\mathrm{vis}} &= \beta \dot{\phi}, \end{aligned} \tag{52}$$

[4] The proof is essentially given by Sansour (2001), Section 3.1.1. Sansour shows rigorously that the stress tensor $\boldsymbol{\Xi} := \boldsymbol{F}^T \boldsymbol{\tau} \boldsymbol{F}^{-T}$, where $\boldsymbol{\tau}$ is the Kirchhoff stress, is conjugate to the logarithmic strain tensor $\boldsymbol{\varepsilon} = \frac{1}{2} \log(\boldsymbol{C})$ when the material is isotropic. This proof is easily adapted to the present case, where we wish to show the Mandel stress $\boldsymbol{M} = \boldsymbol{F}^{eT} \tau \boldsymbol{F}^{e-T}$ is conjugate to the elastic logarithmic strain tensor $\boldsymbol{\varepsilon}^e = \frac{1}{2} \log(\boldsymbol{C}^e)$ under the same isotropic assumption.

where the prime notation on the degradation function indicates ordinary differentiation with respect to the sole argument. From the thermodynamic restriction (24), we find

$$\boldsymbol{\xi} = \frac{3G_c\ell}{4}\boldsymbol{\nabla}\phi. \tag{53}$$

The equilibrium and viscous parts of the flow strength, Y^{eq} and Y^{vis}, are obtained from (21) and (28) once the specific form of the defect energy and the dual kinetic potentials are chosen.

3.4 Degradation functions

The conventional choice for the degradation function is

$$g(\phi) = (1-\phi)^2, \tag{54}$$

as introduced by Bourdin et al. (2000). For the purposes of distinguishing between different functional forms, we shall refer to this as the *quadratic degradation function*. With this choice, the phase field appears at most quadratically in the energy, and the resulting balance law for the phase field becomes a linear partial differential equation.

We also explore a particular version of the degradation function of Lorentz (Cuvilliez et al., 2012; Lorentz et al., 2011, 2012). The family of models developed by Lorentz and co-workers extends the phase field methodology to *cohesive models* of fracture. We adopt the form

$$g(\phi) = \frac{(1-\phi)^2}{(1-\phi)^2 + m\phi(1+p\phi)} \tag{55}$$

where

$$m = \frac{3G_c}{8\ell W_c}, \qquad p = \frac{m}{4} - 1. \tag{56}$$

This *Lorentz degradation function* introduces an additional model parameter, W_c, which has dimensions of energy per unit volume. The parameter W_c is the threshold value of energy density in a homogeneous deformation for damage to nucleate. In a sense, it is similar to the strength parameter in a cohesive model of fracture, although expressed in terms of energy instead of stress. In order for the model to have a continuous dependence of stress on strain, the Lorentz degradation model parameters must satisfy

$$W_c \leq \frac{9G_c}{32\ell}. \tag{57}$$

For the plastic degradation function g^p, we allow for selection of two choices in our implementation. In the first case, we take the plastic degradation function to be identical to the elastic one:

$$g^p(\phi) = g(\phi) \tag{58}$$

An alternative is to neglect plastic contributions to the phase field driving force by taking

$$g^p(\phi) = 1. \tag{59}$$

With this choice, plastic deformation ceases once damage nucleates at a material point. The fracture mechanical implications of making one choice or the other are as yet unexplored.

4 Governing variational principle

In order to find the response of the solid through a loading process, we consider the following scenario. At a given time $t \in [0,T]$, the fields $\{\boldsymbol{\chi}(\boldsymbol{X},t), \phi(\boldsymbol{X},t), \boldsymbol{F}^p(\boldsymbol{X},t), \bar{\varepsilon}^p(\boldsymbol{X},t)\}$ are regarded as known. The generalized velocities

$$\dot{\Lambda} = \{\dot{\boldsymbol{\chi}}(\boldsymbol{X},t), \dot{\phi}(\boldsymbol{X},t), \dot{\boldsymbol{F}}^p(\boldsymbol{X},t), \dot{\bar{\varepsilon}}^p(\boldsymbol{X},t)\}$$

must be solved for using the governing balance equations. The body is subject to essential boundary conditions

$$\dot{\boldsymbol{\chi}}(\boldsymbol{X},t) = \hat{\dot{\boldsymbol{\chi}}}(\boldsymbol{X},t), \quad \text{on } \partial_\chi B_0 \times [0,t_f] \tag{60}$$

$$\dot{\phi}(\boldsymbol{X},t) = \hat{\dot{\phi}}(\boldsymbol{X},t), \quad \text{on } \partial_\phi B_0 \times [0,t_f], \tag{61}$$

and to Neumann boundary conditions

$$\begin{aligned} \boldsymbol{P}\boldsymbol{n}_0 &= \hat{\boldsymbol{t}}_0, \quad \text{on } \partial_t B_0 \times [0,t_f], \\ \boldsymbol{\xi}\cdot\boldsymbol{n}_0 &= \hat{\zeta}_0 \quad \text{on } \partial_\zeta B_0 \times [0,t_f]. \end{aligned} \tag{62}$$

It is assumed that $\{\partial_\chi B_0, \partial_t B_0\}$ and $\{\partial_\phi B_0, \partial_\zeta B_0\}$ each form disjoint partitions of ∂B_0. Introduce the functional

$$\mathcal{I}(\dot{\boldsymbol{\chi}}, \dot{\phi}, \boldsymbol{N}^p, \dot{\bar{\varepsilon}}^p) = \int_{B_0} \left(\dot{\psi} + \Delta^*\right) \mathrm{d}V_0 - L(\dot{\boldsymbol{\chi}}, \dot{\phi}), \tag{63}$$

where

$$L(\dot{\boldsymbol{\chi}}, \dot{\phi}) = \int_{B_0} \boldsymbol{b}_0 \cdot \dot{\boldsymbol{\chi}} \,\mathrm{d}V_0 + \int_{\partial_t B_0} \hat{\boldsymbol{t}}_0 \cdot \dot{\boldsymbol{\chi}} \,\mathrm{d}A_0 + \int_{\partial_\zeta B_0} \hat{\zeta}_0 \dot{\phi} \,\mathrm{d}A_0 \tag{64}$$

is a linear functional representing the power expended by the applied loads. Recall that Δ^* is the collection of the dual kinetic potentials, see (29). The response of the body is determined by the variational principle

$$\begin{aligned} &\inf_{\dot{\boldsymbol{\chi}}, \dot{\phi}, \dot{\bar{\varepsilon}}^p, \boldsymbol{N}^p} \mathcal{I}(\dot{\boldsymbol{\chi}}, \dot{\phi}, \boldsymbol{N}^p, \dot{\bar{\varepsilon}}^p) \\ &\text{subject to} \quad \dot{\bar{\varepsilon}}^p \geq 0 \\ &\qquad\qquad\quad \dot{\phi} \geq 0 \\ &\qquad\qquad\quad \mathrm{tr}(\boldsymbol{N}^p) = 0 \\ &\qquad\qquad\quad \boldsymbol{N}^p : \boldsymbol{N}^p = \frac{3}{2} \end{aligned} \tag{65}$$

As is standard, trial solutions for $\dot{\boldsymbol{\chi}}$ and $\dot{\phi}$ are required to satisfy the Dirichlet boundary conditions.

Remark 4.1. The rationale for choosing the specific form of the objective functional (63) becomes clearer if we compute its first variation. Doing so yields

$$\begin{aligned} \left\langle D\mathcal{I}(\dot{\boldsymbol{\chi}}, \dot{\phi}, \dot{\boldsymbol{F}}^p, \dot{\bar{\varepsilon}}^p), (\tilde{\boldsymbol{\chi}}, \tilde{\phi}, \tilde{\boldsymbol{F}}^p, \tilde{\bar{\varepsilon}}^p) \right\rangle = &\int_{B_0} \left\{ \boldsymbol{P} : \boldsymbol{\nabla}\tilde{\boldsymbol{\chi}} + \boldsymbol{T}^p : \tilde{\boldsymbol{F}}^p + Y\tilde{\bar{\varepsilon}}^p + f\tilde{\phi} + \boldsymbol{\xi}\cdot\boldsymbol{\nabla}\tilde{\phi} \right\} \mathrm{d}V_0 \\ &- \int_{B_0} \boldsymbol{b}_0 \cdot \tilde{\boldsymbol{\chi}} \,\mathrm{d}V_0 - \int_{\partial_t B_0} \hat{\boldsymbol{t}}_0 \cdot \tilde{\boldsymbol{\chi}} \,\mathrm{d}A_0 - \int_{\partial_\zeta B_0} \hat{\zeta}_0 \tilde{\phi} \,\mathrm{d}A_0 \,, \end{aligned}$$

where $(\tilde{\boldsymbol{\chi}}, \tilde{\phi}, \tilde{\boldsymbol{F}}^p, \tilde{\bar{\varepsilon}}^p)$ are admissible variations of the generalized velocity fields (at fixed time t). Comparing this with the assumed forms of power expenditure in Eqs. (10) and (11), the first variation is recognized as the power expended through these varied velocities, or the *virtual power*. Thus the stationarity condition of the objective functional, given by the vanishing of the above equation for all admissible variations, is identified with the *Principle of Virtual Power*, often used by Gurtin and coworkers to derive the balance laws (see, e.g., Gurtin (2002) and Gurtin et al. (2010)). In restricting solutions from all stationary points to infima, we are searching for stable solutions. □

The functional can be rewritten in more detail using the thermodynamic and kinetic identities (20)–(27):

$$\mathcal{I}(\dot{\boldsymbol{\chi}}, \dot{\phi}, \boldsymbol{N}^p, \dot{\bar{\varepsilon}}^p) = \int_{B_0} \left\{ \boldsymbol{P}^{\mathrm{eq}} \colon \boldsymbol{\nabla}\dot{\boldsymbol{\chi}} + \boldsymbol{T}^p \colon (\dot{\bar{\varepsilon}}^p \boldsymbol{N}^p \boldsymbol{F}^p) + Y^{\mathrm{eq}} \dot{\bar{\varepsilon}}^p + f^{\mathrm{eq}} \dot{\phi} + \boldsymbol{\xi} \cdot \boldsymbol{\nabla}\dot{\phi} + \Delta^* \right\} \mathrm{d}V_0 - L(\dot{\boldsymbol{\chi}}),$$

which can be further simplified using Eqs. (46) and (48) to

$$\mathcal{I}(\dot{\boldsymbol{\chi}}, \dot{\phi}, \boldsymbol{N}^p, \dot{\bar{\varepsilon}}^p) = \int_{B_0} \left\{ \boldsymbol{P}^{\mathrm{eq}} \colon \boldsymbol{\nabla}\dot{\boldsymbol{\chi}} + [Y^{\mathrm{eq}} - \boldsymbol{M} \colon \boldsymbol{N}^p]\, \dot{\bar{\varepsilon}}^p + f^{\mathrm{eq}} \dot{\phi} + \boldsymbol{\xi} \cdot \boldsymbol{\nabla}\dot{\phi} + \Delta^* \right\} \mathrm{d}V_0 - L(\dot{\boldsymbol{\chi}}).$$

Since the functional does not involve derivatives of the internal variables, the optimization with respect to these variables may be performed pointwise. To this end, let us label the integrand of the first term

$$\pi(\dot{\boldsymbol{F}}, \dot{\phi}, \boldsymbol{\nabla}\dot{\phi}, \boldsymbol{N}^p, \dot{\bar{\varepsilon}}^p) = \boldsymbol{P}^{\mathrm{eq}} \colon \dot{\boldsymbol{F}} + [Y^{\mathrm{eq}} - \boldsymbol{M} \colon \boldsymbol{N}^p]\, \dot{\bar{\varepsilon}}^p + f^{\mathrm{eq}} \dot{\phi} + \boldsymbol{\xi} \cdot \boldsymbol{\nabla}\dot{\phi} + \Delta^*(\dot{\boldsymbol{F}}, \dot{\phi}, \dot{\bar{\varepsilon}}^p), \tag{66}$$

which we refer to as the *potential density*. Finding the stationary points of π with respect to $\dot{\bar{\varepsilon}}^p$, subject to the constraint $\dot{\bar{\varepsilon}}^p \geq 0$, invokes the Karush-Kuhn-Tucker conditions

$$\begin{aligned} F := -\frac{\partial \pi}{\partial \dot{\bar{\varepsilon}}^p} = \boldsymbol{M} \colon \boldsymbol{N}^p - (Y^{\mathrm{eq}} + Y^{\mathrm{vis}}) \leq 0, \\ \dot{\bar{\varepsilon}}^p \geq 0, \\ F \dot{\bar{\varepsilon}}^p = 0, \end{aligned} \tag{67}$$

which are recognized as the yield surface and loading/unloading conditions. Optimization of π with respect to $\boldsymbol{N}^p$, subject to the constraints (2) (using, say, Lagrange multipliers) obtains

$$\boldsymbol{N}^p = \sqrt{\frac{3}{2}} \frac{\mathrm{dev}(\boldsymbol{M})}{\|\mathrm{dev}(\boldsymbol{M})\|}, \tag{68}$$

which coincides with the flow direction prescribed by the maximum dissipation principle. As an aside, we can use this to define the effective stress

$$\bar{\sigma} := \boldsymbol{M} \colon \boldsymbol{N}^p = \sqrt{\frac{3}{2}} \|\mathrm{dev}(\boldsymbol{M})\|, \tag{69}$$

which shows that the yield surface is the classical Mises yield surface, defined with respect to the Mandel stress. Using Eqs. (68) and (69) in Eq. (1) gives

$$\dot{\boldsymbol{F}}^p \boldsymbol{F}^{p-1} = \dot{\bar{\varepsilon}}^p \frac{3\,\mathrm{dev}(\boldsymbol{M})}{2\bar{\sigma}}, \tag{70}$$

which is the finite deformation counterpart of the classical Lévy-Mises-Prandtl-Reuss flow rule.

Remark 4.2. In the case $g^p(\phi) = g(\phi)$, the yield equations take a simple form that is independent of the phase field. Let us define

$$\widetilde{Y}^{\mathrm{eq}}(\bar{\varepsilon}^p) = \frac{\partial \widetilde{\psi}^p}{\partial \bar{\varepsilon}^p}, \qquad\qquad \widetilde{Y}^{\mathrm{vis}}(\dot{\bar{\varepsilon}}^p) = \frac{\partial \widetilde{\Phi}}{\partial \dot{\bar{\varepsilon}}^p},$$

which may be thought of as the undamaged flow stress and undamaged viscous over-stress, and

$$\widetilde{\boldsymbol{M}} = \frac{\partial \widetilde{\psi}^e(\boldsymbol{\varepsilon}^e)}{\partial \boldsymbol{\varepsilon}^e} \qquad\qquad \widetilde{\bar{\sigma}} = \sqrt{3/2} \left\| \mathrm{dev}\, \widetilde{\boldsymbol{M}} \right\|$$

which represents the undamaged Mandel stress and the undamaged effective stress. The yield equation (67)a can be written

$$g(\phi) \widetilde{\bar{\sigma}} - g^p(\phi) \left(\widetilde{Y}^{\mathrm{eq}} + \widetilde{Y}^{\mathrm{vis}} \right) = 0,$$

and when $g^p(\phi) = g(\phi)$, the degradation function factors cancel:

$$\widetilde{\bar{\sigma}} - \left(\widetilde{Y}^{\mathrm{eq}} + \widetilde{Y}^{\mathrm{vis}}\right) = 0.$$

The yield equation is then identical to that of the intact material model. This can be exploited in an implementation to re-use the plastic strain solution routine from a conventional plasticity model. Note also that the flow direction tensor $\boldsymbol{N}^p$ defined in (68) is equivalent to the intact material model definition

$$\boldsymbol{N}^p = \sqrt{\frac{3}{2}}\frac{\operatorname{dev}\widetilde{\boldsymbol{M}}}{\left\|\operatorname{dev}\widetilde{\boldsymbol{M}}\right\|},$$

and hence this can be re-used from a conventional model implementation as well. □

At this point, through partial optimzations, we have defined the effective function

$$\pi^{\mathrm{eff}}(\dot{\boldsymbol{F}}, \dot{\phi}, \boldsymbol{\nabla}\dot{\phi}) = \inf_{\dot{\bar{\varepsilon}}^p, \boldsymbol{N}^p} \pi(\dot{\boldsymbol{F}}, \dot{\phi}, \boldsymbol{\nabla}\dot{\phi}, \boldsymbol{N}^p, \dot{\bar{\varepsilon}}^p) \tag{71}$$

which acts as a potential for the generalized forces, in the sense that

$$\boldsymbol{P} = \frac{\partial \pi^{\mathrm{eff}}}{\partial \dot{\boldsymbol{F}}} = \frac{\partial \psi}{\partial \boldsymbol{F}} + \frac{\partial R^*}{\partial \dot{\boldsymbol{F}}}, \tag{72}$$

$$f = \frac{\partial \pi^{\mathrm{eff}}}{\partial \dot{\phi}} = \frac{\partial \psi}{\partial \phi} + \frac{\partial \Phi^*}{\partial \dot{\phi}}, \tag{73}$$

$$\boldsymbol{\xi} = \frac{\partial \pi^{\mathrm{eff}}}{\partial \boldsymbol{\nabla}\dot{\phi}} = \frac{\partial \psi}{\partial \boldsymbol{\nabla}\phi}. \tag{74}$$

The variational principle (65) reduces to

$$\begin{aligned} \inf_{\dot{\boldsymbol{\chi}}, \dot{\phi}} \mathcal{I}^{\mathrm{eff}}(\dot{\boldsymbol{\chi}}, \dot{\phi}) = \int_{B_0} \pi^{\mathrm{eff}}(\boldsymbol{\nabla}\dot{\boldsymbol{\chi}}, \dot{\phi}, \boldsymbol{\nabla}\dot{\phi})\, \mathrm{d}V_0 - L(\dot{\boldsymbol{\chi}}, \dot{\phi}) \\ \text{subject to} \quad \dot{\phi} \geq 0, \end{aligned} \tag{75}$$

which determines the fields $\{\dot{\boldsymbol{\chi}}, \dot{\phi}\}$ at time t, completing the solution of the problem. Problem (75) is taken as the basis of the finite element discretization of the balance laws; while discretization of (71) furnishes the constitutive update algorithm.

Although not necessary for the numerical implementation, we record the strong form implied by the variational principle for reference. The vanishing of the reduced objective functional (75) with respect to variations in $\dot{\boldsymbol{\chi}}$ gives

$$\begin{aligned} \boldsymbol{\nabla}\cdot\boldsymbol{P} + \boldsymbol{b}_0 = \boldsymbol{0} \quad &\text{in } B_0, \\ \boldsymbol{P}\hat{\boldsymbol{N}}\cdot\dot{\boldsymbol{\chi}} = \hat{\boldsymbol{t}}_0 \quad &\text{on } \partial_t B_0, \end{aligned} \tag{76}$$

which is the classical force balance and the associated traction boundary conditions. Next, we deduce the Euler-Lagrange equation associated with the phase field rate. We wish to see the form of the PDE and boundary conditions, so let us formally take the variation with respect to $\dot{\phi}$ and set it to zero, setting aside the irreversibility constraint (5) for the moment. Upon integration by parts, we find

$$\begin{aligned} \boldsymbol{\nabla}\cdot\boldsymbol{\xi} - f^{\mathrm{eq}} = f^{\mathrm{vis}} \quad &\text{in } B_0, \\ \boldsymbol{\xi}\cdot\hat{\boldsymbol{N}} = \hat{\zeta}_0 \quad &\text{on } \partial_\zeta B_0. \end{aligned} \tag{77}$$

The first of (77) can be put in a more familiar form by substituting in the constitutive equations (52) and (53) to yield

$$\boldsymbol{\nabla}\cdot\left(\frac{3G_c\ell}{4}\boldsymbol{\nabla}\phi\right) - \frac{\partial\psi}{\partial\phi} = \beta\dot{\phi},$$

which is the Allen-Cahn equation, with the phase field playing the role of the non-conserved order parameter.

5 Discretization

The system is discretized in time through an incremental solution procedure. Let $t_0, t_1, \ldots, T$ be discrete sample points in time. In what follows, we shall follow the convention that the discrete time point at which field quantities are evaluated are indexed with a subscript; i.e., $\boldsymbol{\chi}_n(\boldsymbol{X}) = \boldsymbol{\chi}(\boldsymbol{X}, t_n)$. At a given time step t_n, the fields $\{\boldsymbol{\chi}_n(\boldsymbol{X}), \phi_n(\boldsymbol{X}), \boldsymbol{F}^p_n(\boldsymbol{X}), \bar{\varepsilon}^p_n(\boldsymbol{X})\}$ are known. The task is to formulate a consistent discretization of the field equations to determine $\{\boldsymbol{\chi}_{n+1}(\boldsymbol{X}), \phi_{n+1}(\boldsymbol{X}), \boldsymbol{F^p}_{n+1}(\boldsymbol{X}), \bar{\varepsilon}^p_{n+1}(\boldsymbol{X})\}$. We build the discrete approximation upon the minimum principle. The starting point is a backward Euler finite difference approximation of the potential function (66):

$$W_n(\Lambda_{n+1}; \Lambda_n) = \psi(\boldsymbol{F}_{n+1}, \phi_{n+1}, \boldsymbol{\nabla}\phi_{n+1}, \boldsymbol{F^p}_{n+1}, \bar{\varepsilon}^p_{n+1}) - \psi(\boldsymbol{F}_n, \phi_n, \boldsymbol{\nabla}\phi_n, \boldsymbol{F}^p_n, \bar{\varepsilon}^p_n) + \Delta t\, \Delta^*\left(\frac{\Delta \boldsymbol{F}}{\Delta t}, \frac{\Delta\phi}{\Delta t}, \frac{\Delta\bar{\varepsilon}^p}{\Delta t}; \boldsymbol{F}_n, \phi_n\right), \quad (78)$$

where

$$\begin{aligned} \Delta t &= t_{n+1} - t_n \\ \Delta \boldsymbol{F} &= \boldsymbol{F}_{n+1} - \boldsymbol{F}_n, \\ \Delta\phi &= \phi_{n+1} - \phi_n. \\ \Delta\bar{\varepsilon}^p &= \bar{\varepsilon}^p_{n+1} - \bar{\varepsilon}^p_n, \end{aligned} \quad (79)$$

The flow rule is discretized with the exponential integration rule (see Weber and Anand, 1990))

$$\boldsymbol{F^p}_{n+1} = \exp(\Delta\bar{\varepsilon}^p_{n+1} \boldsymbol{N}^p_{n+1}) \boldsymbol{F}^p_n. \quad (80)$$

With these, we define the discrete functional

$$\mathcal{I}_n(\boldsymbol{\chi}_{n+1}, \phi_{n+1}, \boldsymbol{N}^p_{n+1}, \bar{\varepsilon}^p_{n+1}) = \int_{B_0} W_n(\boldsymbol{\nabla}\boldsymbol{\chi}_{n+1}, \phi_{n+1}, \boldsymbol{\nabla}\phi_{n+1}, \boldsymbol{N}^p_{n+1}, \bar{\varepsilon}^p_{n+1})\, \mathrm{d}V_0 - L(\boldsymbol{\chi}_{n+1} - \boldsymbol{\chi}_n, \phi_{n+1} - \phi_n). \quad (81)$$

The field equations evolving the system from $t_n \to t_{n+1}$ follow from the discrete minimum principle

$$\begin{aligned} &\inf_{\boldsymbol{\chi}_{n+1}, \phi_{n+1}, \boldsymbol{N}^p_{n+1}, \bar{\varepsilon}^p_{n+1}} \mathcal{I}_n(\boldsymbol{\chi}_{n+1}, \phi_{n+1}, \boldsymbol{N}^p_{n+1}, \bar{\varepsilon}^p_{n+1}) \\ &\text{subject to } \phi_{n+1} - \phi_n \geq 0 \\ &\qquad \bar{\varepsilon}^p_{n+1} - \bar{\varepsilon}^p_n \geq 0 \\ &\qquad \mathrm{tr}(\boldsymbol{N}^p_{n+1}) = 0 \\ &\qquad \boldsymbol{N}^p_{n+1} : \boldsymbol{N}^p_{n+1} - \frac{3}{2} = 0 \end{aligned} \quad (82)$$

As before, the optimzation can be logically split into two stages. The first stage is pointwise optimization with respect to the internal variables,

$$\begin{aligned} W^{\mathrm{eff}}_n(\boldsymbol{F}_{n+1}, \phi_{n+1}) = &\inf_{\boldsymbol{N}^p_{n+1}, \bar{\varepsilon}^p_{n+1}} W_n(\boldsymbol{F}_{n+1}, \phi_{n+1}, \boldsymbol{\nabla}\phi_{n+1}, \boldsymbol{N}^p_{n+1}, \bar{\varepsilon}^p_{n+1}; \Lambda_n), \\ &\text{such that } \Delta\bar{\varepsilon}^p \geq 0, \quad \mathrm{tr}(\boldsymbol{N}^p_{n+1}) = 0, \quad \boldsymbol{N}^p_{n+1} : \boldsymbol{N}^p_{n+1} - \frac{3}{2} = 0 \end{aligned} \quad (83)$$

which represents the constitutive update algorithm. This algorithm is discussed in detail in Section 5.1.

The fields ϕ_{n+1} and $\boldsymbol{\chi}_{n+1}$ are discretized in space with finite elements. Their solution follows from the second stage of the optimization,

$$\begin{aligned} &\inf_{\boldsymbol{\chi}_{n+1}, \phi_{n+1}} \mathcal{I}^{\mathrm{eff}}_n(\boldsymbol{\chi}_{n+1}, \phi_{n+1}) \\ &\text{subject to } \phi_{n+1} - \phi_n \geq 0 \end{aligned} \quad (84)$$

where

$$\mathcal{I}_n^{\text{eff}}(\boldsymbol{\chi}_{n+1}, \phi_{n+1}) = \int_{B_0} W_n^{\text{eff}}(\boldsymbol{\nabla}\boldsymbol{\chi}_{n+1}, \phi_{n+1}, \boldsymbol{\nabla}\phi_{n+1})\,\mathrm{d}V_0 - L(\boldsymbol{\chi}_{n+1} - \boldsymbol{\chi}_n, \phi_{n+1} - \phi_n). \tag{85}$$

We discuss this stage of the discretization in Section 5.2.

5.1 Constitutive update

In this section, we show that the optimization of the potential density function W_n is really the classical radial return algorithm. First, let us write the potential density in terms of the constitutive assumptions:

$$\begin{aligned} W_n(\Lambda_{n+1}; \Lambda_n) = \psi^e(\boldsymbol{\varepsilon}^e_{n+1}, \phi_{n+1}) + \psi^p(\bar{\varepsilon}^p_{n+1}, \phi_{n+1}) + \psi^f(\phi_{n+1}, \boldsymbol{\nabla}\phi_{n+1}) \\ - \Big(\psi^e(\boldsymbol{\varepsilon}^e_n, \phi_n) + \psi^p(\bar{\varepsilon}^p_n, \phi_n) + \psi^f(\phi_n, \boldsymbol{\nabla}\phi_n)\Big) \\ + \Delta t \left[R^*\left(\frac{\Delta \boldsymbol{F}}{\Delta t}; \boldsymbol{F}_n, \phi_n\right) + \Delta\Phi^*\left(\frac{\Delta\phi}{\Delta t}\right) + \Pi^*\left(\frac{\Delta\bar{\varepsilon}^p}{\Delta t}; \phi_n\right)\right]. \end{aligned} \tag{86}$$

Using the discrete update of the plastic distortion (80), we can write the updated elastic distortion as

$$\boldsymbol{F}^e{}_{n+1} = \underbrace{\boldsymbol{F}_{n+1}\boldsymbol{F}_n^{p\,-1}}_{\boldsymbol{F}^{e,tr}} \exp(-\Delta\bar{\varepsilon}^p \boldsymbol{N}^p_{n+1}), \tag{87}$$

where the tensor $\boldsymbol{F}^{e,tr}$ is the *elastic trial* value of the elastic distortion; that is, the elastic distortion that would result if no plastic flow takes place over the time step. We can use this to define

$$\begin{aligned} \boldsymbol{C}^e_{n+1} &= \boldsymbol{F}^e{}_{n+1}{}^T \boldsymbol{F}^e{}_{n+1} && (88)\\ &= \exp(-\Delta\bar{\varepsilon}^p \boldsymbol{N}^p_{n+1}) \boldsymbol{C}^{e,tr} \exp(-\Delta\bar{\varepsilon}^p \boldsymbol{N}^p_{n+1}). && (89) \end{aligned}$$

Let us provisionally assume, subject to later verification, that $\boldsymbol{N}^p_{n+1}$ and $\boldsymbol{C}^{e,tr}$ commute. Then

$$\boldsymbol{C}^e_{n+1} = \boldsymbol{C}^{e,tr} \exp(-2\Delta\bar{\varepsilon}^p \boldsymbol{N}^p_{n+1}),$$

and the logarithmic elastic strain is

$$\boldsymbol{\varepsilon}^e_{n+1} = \boldsymbol{\varepsilon}^{e,tr} - \Delta\bar{\varepsilon}^p_{n+1} \boldsymbol{N}^p_{n+1}, \tag{90}$$

where have made the self-evident definition

$$\boldsymbol{\varepsilon}^{e,tr} = \frac{1}{2}\log\Big(\boldsymbol{C}^{e,tr}\Big). \tag{91}$$

This *trial strain* defines a conjugate trial stress

$$\boldsymbol{\Sigma}^{tr} = \frac{\partial \psi^e}{\partial \boldsymbol{\varepsilon}^{e,tr}} = g(\phi_{n+1}) \left[2\mu\,\mathrm{dev}\,\boldsymbol{\varepsilon}^{e,tr} + \kappa\,\mathrm{tr}\Big(\boldsymbol{\varepsilon}^{e,tr}\Big)\mathbf{1}\right].$$

The $\boldsymbol{N}^p_{n+1}$ that minimizes W_n and satisfies the constraints is found by finding the stationary points of the Lagrangian

$$L = W_n + \lambda_a\,\mathrm{tr}(\boldsymbol{N}^p_{n+1}) + \lambda_b\left(\boldsymbol{N}^p_{n+1} \colon \boldsymbol{N}^p_{n+1} - \frac{3}{2}\right),$$

where λ_a and λ_b are Lagrange multipliers. Compute the partial derivative

$$\begin{aligned} \frac{\partial W_n}{\partial \boldsymbol{N}^p_{n+1}} &= \frac{\partial \psi^e}{\partial \boldsymbol{\varepsilon}^e_{n+1}} \colon \frac{\partial \boldsymbol{\varepsilon}^e_{n+1}}{\partial \boldsymbol{N}^p_{n+1}} \\ &= \Big(\boldsymbol{\Sigma}^{tr} - 2\mu g(\phi)\Delta\bar{\varepsilon}^p \boldsymbol{N}^p_{n+1} - \kappa g(\phi)\Delta\bar{\varepsilon}^p\,\mathrm{tr}(\boldsymbol{N}^p_{n+1})\mathbf{1}\Big) : (-\Delta\bar{\varepsilon}^p \mathbb{I}) \\ &= \Delta\bar{\varepsilon}^p \Big(-\boldsymbol{\Sigma}^{tr} + 2g(\phi)\mu\Delta\bar{\varepsilon}^p \boldsymbol{N}^p_{n+1} + g(\phi)\kappa\Delta\bar{\varepsilon}^p\,\mathrm{tr}(\boldsymbol{N}^p_{n+1})\mathbf{1}\Big), \end{aligned}$$

where $\mathbb{I}$ is the fourth order identity tensor, with components $(\mathbb{I})_{ijkl} = \delta_{ik}\delta_{jl}$. It may be readily verified that the stationary point we are searching for is

$$\lambda_a = \frac{1}{3}\Delta\bar{\varepsilon}^p \operatorname{tr}\Big(\boldsymbol{\Sigma}^{tr}\Big), \qquad \lambda_b = \frac{1}{3}\Delta\bar{\varepsilon}^p \left(\operatorname{dev}\boldsymbol{\Sigma}^{tr} : \boldsymbol{N}^p_{n+1} - 3g(\phi)\mu\Delta\bar{\varepsilon}^p\right), \tag{92}$$

$$\boldsymbol{N}^p_{n+1} = \frac{3}{2}\frac{\operatorname{dev}\boldsymbol{\Sigma}^{tr}}{\bar{\sigma}^{tr}}, \tag{93}$$

where we have introduced the effective stress

$$\bar{\sigma}^{tr} = \sqrt{3/2}\Big\|\operatorname{dev}\boldsymbol{\Sigma}^{tr}\Big\|. \tag{94}$$

In writing these equations, it is assumed that $\Delta\bar{\varepsilon}^p \neq 0$. (In the case that $\Delta\bar{\varepsilon}^p$ is zero, there is no plastic flow, and the flow direction tensor is not needed in any part of the update.) From (93), the proposition that $\boldsymbol{N}^p_{n+1}$ and $\boldsymbol{C}^{e,tr}$ commute may now be verified. By the assumed isotropic character of the strain energy density function, $\boldsymbol{\Sigma}^{tr}$ has the same eigenbasis as $\boldsymbol{\varepsilon}^{e,tr}$, and from the definition of the tensor logarithm, $\boldsymbol{C}^{e,tr}$ also shares this eigenbasis. From (93) it is then apparent that $\boldsymbol{N}^p_{n+1}$ also shares this common eigenbasis, and therefore commutes with $\boldsymbol{C}^{e,tr}$.

Next, we optimize with respect to $\bar{\varepsilon}^p_{n+1}$. Let

$$F(\Delta\bar{\varepsilon}^p_{n+1}) := -\frac{\partial W_n}{\partial\bar{\varepsilon}^p_{n+1}} = -\frac{\partial\psi^e}{\partial\boldsymbol{\varepsilon}^e_{n+1}} : \frac{\partial\boldsymbol{\varepsilon}^e_{n+1}}{\partial\bar{\varepsilon}^p_{n+1}} - \frac{\partial\psi^p}{\partial\bar{\varepsilon}^p_{n+1}} - \frac{\partial\Phi^*}{\partial\dot{\bar{\varepsilon}}^p}.$$

Insert the constitutive relations (47), (21), and (28), to get

$$F(\Delta\bar{\varepsilon}^p) = -\Big(\boldsymbol{\Sigma}^{tr} - 2g(\phi)\mu\Delta\bar{\varepsilon}^p\boldsymbol{N}^p_{n+1} - g(\phi)\kappa\Delta\bar{\varepsilon}^p \operatorname{tr}(\boldsymbol{N}^p_{n+1})\mathbf{1}\Big) : (-\boldsymbol{N}^p_{n+1}) - Y^{\mathrm{eq}} - Y^{\mathrm{vis}}.$$

Now use the constraints (2) on $\boldsymbol{N}^p_{n+1}$ to get

$$F(\Delta\bar{\varepsilon}^p) = \operatorname{dev}\boldsymbol{\Sigma}^{tr} : \boldsymbol{N}^p_{n+1} - 3g(\phi)\mu\Delta\bar{\varepsilon}^p - Y^{\mathrm{eq}} - Y^{\mathrm{vis}},$$

or, in light of (94),

$$F(\Delta\bar{\varepsilon}^p) = \bar{\sigma}^{tr} - 3g(\phi)\mu\Delta\bar{\varepsilon}^p - Y^{\mathrm{eq}}(\bar{\varepsilon}^p_n + \Delta\bar{\varepsilon}^p; \phi_{n+1}) - Y^{\mathrm{vis}}\left(\frac{\Delta\bar{\varepsilon}^p}{\Delta t}; \phi_n\right), \tag{95}$$

which is the algorithmic counterpart of (67). The classical predictor-corrector method is employed to find the optimizing $\Delta\bar{\varepsilon}^p$: first, the value of $F(0)$ is investigated. If $F(0) \leq 0$, then $\Delta\bar{\varepsilon}^p = 0$. Otherwise, $F(0) > 0$, and it must be true that $\Delta\bar{\varepsilon}^p > 0$. In this case, we must have

$$F(\Delta\bar{\varepsilon}^p) = 0,$$

which is solved iteratively for the value of $\Delta\bar{\varepsilon}^p$.

Remark 5.1. If a spectral decomposition method is used to compute $\log(\boldsymbol{C}^{e,tr})$, then the update of $\boldsymbol{F}^p$ can be computed with little additional expense. From the spectral decomposition of $\log(\boldsymbol{C}^{e,tr})$, one has the matrix whose columns are the eigenvectors of $\boldsymbol{C}^{e,tr}$, call it $\mathfrak{R}^e$, and the set of eigenvalues of $\boldsymbol{C}^{e,tr}$, call

them $\left\{\left(\lambda_1^{e,tr}\right)^2, \left(\lambda_2^{e,tr}\right)^2, \left(\lambda_3^{e,tr}\right)^2\right\}$. Then

$$\begin{aligned}
\exp(\Delta\bar{\varepsilon}^p \boldsymbol{N}^p_{n+1}) &= \exp\left(\Delta\bar{\varepsilon}^p \frac{3\,\mathrm{dev}(\boldsymbol{\Sigma}^{tr})}{2\bar{\sigma}^{tr}}\right) \\
&= \exp\left(\frac{3g(\phi)\mu\Delta\bar{\varepsilon}^p}{\bar{\sigma}^{tr}}\,\mathrm{dev}(\boldsymbol{\varepsilon}^{e,tr})\right) \\
&= \left[\exp\left(\mathrm{dev}(\boldsymbol{\varepsilon}^{e,tr})\right)\right]^{\frac{3g(\phi)\mu\Delta\bar{\varepsilon}^p}{\bar{\sigma}^{tr}}} \\
&= \left[\exp\left(\log\left(J^{-2/3}\boldsymbol{C}^{e,tr}\right)\right)\right]^{\frac{3g(\phi)\mu\Delta\bar{\varepsilon}^p}{2\bar{\sigma}^{tr}}} \\
&= (J^{-2/3}\boldsymbol{C}^{e,tr})^{\frac{3g(\phi)\mu\Delta\bar{\varepsilon}^p}{2\bar{\sigma}^{tr}}} \\
&= \left(J^{-1/3}\sqrt{\boldsymbol{C}^{e,tr}}\right)^{\frac{3g(\phi)\mu\Delta\bar{\varepsilon}^p}{\bar{\sigma}^{tr}}}
\end{aligned}$$

The simplification of $\exp(\Delta\bar{\varepsilon}^p \boldsymbol{N}^p_{n+1})$ is due to the fact that the logarithmic operator in the definition of the strain measure is inverse to the exponential operator in the integration scheme. Let $z = 3g(\phi)\mu\Delta\bar{\varepsilon}^p/\bar{\sigma}^{tr}$. Then

$$\exp(\Delta\bar{\varepsilon}^p \boldsymbol{N}^p_{n+1}) = J^{\frac{-z}{3}}\mathfrak{R}^e\,\mathrm{diag}\left(\left(\lambda_1^{e,tr}\right)^z, \left(\lambda_2^{e,tr}\right)^z, \left(\lambda_3^{e,tr}\right)^z\right)\mathfrak{R}^{eT},$$

which avoids the overhead of an additional spectral decomposition to compute the matrix exponential. □

The optimization of the potential density is complete at this stage. The effective potential density W_n^{eff} is computed by evaluating (86) at the updated values of $\bar{\varepsilon}^p_{n+1}$ and $\boldsymbol{N}^p_{n+1}$. The effective potential density can then be seen to satisfy

$$\boldsymbol{P}_{n+1} = \frac{\partial W_n^{\mathrm{eff}}}{\partial \boldsymbol{F}_{n+1}}, \qquad f_{n+1} = \frac{\partial W_n^{\mathrm{eff}}}{\partial \phi_{n+1}}, \qquad \boldsymbol{\xi}_{n+1} = \frac{\partial W_n^{\mathrm{eff}}}{\partial \boldsymbol{\nabla}\phi_{n+1}}. \tag{96}$$

These can be given in more explicit terms. As noted before, the Mandel stress is equal to the stress conjugate to the logarithmic elastic strain under the present assumption of isotropic behavior. Therefore

$$\boldsymbol{M}_{n+1} = \boldsymbol{\Sigma}^{tr} - 2\mu\Delta\bar{\varepsilon}^p g(\phi_{n+1})\boldsymbol{N}^p_{n+1}, \tag{97}$$

and, repeating Eq. (50), the equilibrium part of the Piola stress is

$$\boldsymbol{P}^{\mathrm{eq}}_{n+1} = \boldsymbol{F}^{e-T}_{n+1}\boldsymbol{M}_{n+1}\boldsymbol{F}^{p-T}_{n+1}.$$

An additional minor simplification may be made by noting that $\boldsymbol{M}_{n+1}$ and $\boldsymbol{N}^p_{n+1}$ commute in the present case of isotropic elasticity, allowing us to write

$$\boldsymbol{P}^{\mathrm{eq}}_{n+1} = \boldsymbol{F}^{e,tr\,-T}\boldsymbol{M}_{n+1}\boldsymbol{F}^{p\,-T}_{n}. \tag{98}$$

The viscous part of the Piola stress is

$$\boldsymbol{P}^{\mathrm{vis}}_{n+1} = (1-\phi_n)^2 J_n \frac{\partial \widetilde{R}^*}{\partial \dot{\boldsymbol{F}}} = (1-\phi_n)^2 J_n \left[2\eta\,\mathrm{dev}\left(\mathrm{sym}\left(\frac{\Delta \boldsymbol{F}}{\Delta t}\right)\right)\right]\boldsymbol{F}^{-T}_{n+1}, \tag{99}$$

which follows directly from Eq. (51) and the discretization of the dual kinetic potential in Eq. (78). The updated Piola stress is

$$\boldsymbol{P}_{n+1} = \boldsymbol{P}^{\mathrm{eq}}_{n+1} + \boldsymbol{P}^{\mathrm{vis}}_{n+1}. \tag{100}$$

The generalized force conjugate to the phase is

$$f_{n+1} = f^{\text{eq}}_{n+1} + f^{\text{vis}}_{n+1} \tag{101}$$

with

$$f^{\text{eq}}_{n+1} = \frac{3G_c}{8\ell} + g'(\phi_{n+1})\widetilde{\psi}^e(\boldsymbol{\varepsilon}^e_{n+1}) + g^{p\prime}(\phi_{n+1})\widetilde{\psi}^p(\bar{\varepsilon}^p_{n+1}), \tag{102}$$

and

$$f^{\text{vis}}_{n+1} = \beta\frac{\phi_{n+1} - \phi_n}{\Delta t}. \tag{103}$$

It bears mention that to choose rate-independent phase field behavior, it suffices to take $\beta = 0$. Finally,

$$\boldsymbol{\xi}_{n+1} = \frac{3G_c\ell}{4}\boldsymbol{\nabla}\phi_{n+1}. \tag{104}$$

5.1.1 Tangent operator of constitutive laws

When applying minimization algorithms to the outer problem of finding the phase field and the deformation, some algorithms require the consistent tangent operators of the constitutive laws. The tangent operator is given by

$$D^2W^{\text{eff}}_n = \begin{pmatrix} W^{\text{eff}}_{n\ ,\boldsymbol{F}_{n+1}\boldsymbol{F}_{n+1}} & W^{\text{eff}}_{n\ ,\boldsymbol{F}_{n+1}\phi_{n+1}} & W^{\text{eff}}_{n\ ,\boldsymbol{F}_{n+1}\boldsymbol{\nabla}\phi_{n+1}} \\ & W^{\text{eff}}_{n\ ,\phi_{n+1}\phi_{n+1}} & W^{\text{eff}}_{n\ ,\phi_{n+1}\boldsymbol{\nabla}\phi_{n+1}} \\ \text{sym} & & W^{\text{eff}}_{n\ ,\boldsymbol{\nabla}\phi_{n+1}\boldsymbol{\nabla}\phi_{n+1}} \end{pmatrix}. \tag{105}$$

By inspection, several elements are found to be zero:

$$W^{\text{eff}}_{n\ ,\boldsymbol{F}_{n+1}\boldsymbol{\nabla}\phi_{n+1}} = \boldsymbol{0} \qquad W^{\text{eff}}_{n\ ,\phi_{n+1}\boldsymbol{\nabla}\phi_{n+1}} = \boldsymbol{0}$$

For the remaining elements, we have

$$\frac{\partial\bar{\varepsilon}^p_{n+1}}{\partial\phi_{n+1}} = \frac{g'(\phi_{n+1})\tilde{\bar{\sigma}}_{n+1} - g^{p\prime}(\phi_{n+1})\tilde{Y}^{\text{eq}}}{3g(\phi_{n+1})\mu + H^{\text{eq}} + H^{\text{vis}}}$$

$$W^{\text{eff}}_{n\ ,\phi_{n+1}\phi_{n+1}} = g''(\phi_{n+1})\widetilde{\psi}^e + g^{p\prime\prime}(\phi_{n+1})\widetilde{\psi}^p + \frac{\beta}{\Delta t} + \left[g^{p\prime}(\phi_{n+1})\widetilde{Y}^{\text{eq}} - g'(\phi_{n+1})\tilde{\bar{\sigma}}_{n+1}\right]\frac{\partial\bar{\varepsilon}^p_{n+1}}{\partial\phi_{n+1}} \tag{106}$$

$$W^{\text{eff}}_{n\ ,\boldsymbol{\nabla}\phi_{n+1}\boldsymbol{\nabla}\phi_{n+1}} = \frac{3G_c\ell}{4}\boldsymbol{1} \tag{107}$$

$$W^{\text{eff}}_{n\ ,\boldsymbol{F}_{n+1}\phi_{n+1}} = g'(\phi_{n+1})\boldsymbol{F}^{e,tr-T}\widetilde{\boldsymbol{M}}_{n+1}\boldsymbol{F}^{p-T}_n - 2\mu g(\phi_{n+1})\frac{\partial\bar{\varepsilon}^p_{n+1}}{\partial\phi_{n+1}}\boldsymbol{F}^{e,tr-T}\boldsymbol{N}^p_{n+1}\boldsymbol{F}^{p-T}_n \tag{108}$$

Remark 5.2. For Gary and John: the remaining term is $W^{\text{eff}}_{n\ ,\boldsymbol{F}_{n+1}\boldsymbol{F}_{n+1}}$. I have derived this term and verified it through unit tests, but my only record of it is the implementation in Matlab. I'm willing to transcribe it if desired, but I will defer this work until needed. □

5.2 Spatial discretization of balance laws

The global fields are discretized in space by introducing a triangulation $\mathcal{T}_h$ of B_0, and corresponding finite element interpolations of the fields

$$\boldsymbol{\chi}_n = \sum_{a=1}^{n_x} N^a(\boldsymbol{X})\boldsymbol{x}^a_n, \qquad \phi_n = \sum_{a=1}^{n_\phi} \mathcal{N}^a(\boldsymbol{X})\phi^a_n, \tag{109}$$

where n_x is the number of nodes for the deformation interpolation, the N^a are the shape functions for the deformation, and $\boldsymbol{x}^a_n$ are the nodal values of the deformed coordinates. The respective quantities for

the phase field are n_ϕ, $\mathcal{N}^a$, and ϕ^a_n. It is assumed that the triangulation for both fields are the same, but different discrete function spaces may be used.

The spatially discrete objective functional is found by evaluating the time discrete functional (85) using the spatial interpolations (109), giving

$$\mathcal{I}^{\text{eff}}_n(\mathbf{x}_{n+1},\boldsymbol{\phi}_{n+1}) = \int_{B_0} W^{\text{eff}}_n(\boldsymbol{\nabla}\boldsymbol{\chi}_{n+1},\phi_{n+1},\boldsymbol{\nabla}\phi_{n+1})\,\mathrm{d}V_0 + L(\boldsymbol{\chi}_{n+1}-\boldsymbol{\chi}_n,\phi_{n+1}-\phi_n) \tag{110}$$

where $\mathbf{x}_{n+1} = \{\boldsymbol{x}^a_{n+1}, a = 1,2,\ldots n_x\}$ is the array of the nodal coordinates in the deformed configuration, and $\boldsymbol{\phi} = \{\phi^a_{n+1}, a = 1,2,\ldots n_\phi\}$ is the array of the nodal phase field values. The optimization problem is now finite dimensional, and the classical Rayleigh-Ritz method can be used to find stationary points. The gradient of the discrete functional is the $(n_x + n_\phi)\times 1$ matrix

$$D\mathcal{I}^{\text{eff}}_n = \begin{bmatrix}\mathbf{r}_x\\ \mathbf{r}_\phi\end{bmatrix}$$

where

$$\begin{aligned}(r_x)_{ai} &= \left(\frac{\partial\mathcal{I}^{\text{eff}}_n}{\partial\mathbf{x}_{n+1}}\right)_{ai} = \int_{B_0} P_{iJ}N_{a,J}\,\mathrm{d}V_0 - \int_{\partial_t B_0}\hat{t}_{0i}N_a\,\mathrm{d}A_0 + \int_{B_0} b_{0i}N_a\,\mathrm{d}V_0\\ (r_\phi)_c &= \left(\frac{\partial\mathcal{I}^{\text{eff}}_n}{\partial\boldsymbol{\phi}_{n+1}}\right)_c = \int_{B_0}(f\mathcal{N}_c + \xi_I\mathcal{N}_{c,I})\,\mathrm{d}V_0 - \int_{\partial_\zeta B_0}\hat{\zeta}_0\mathcal{N}_c\,\mathrm{d}A_0\,.\end{aligned} \tag{111}$$

Some optimization algorithms require the Hessian matrix

$$D^2\mathcal{I}^{\text{eff}}_n = \begin{bmatrix}\mathbf{K}_{xx} & \mathbf{K}_{x\phi}\\ \mathbf{K}^T_{x\phi} & \mathbf{K}_{\phi\phi}\end{bmatrix}, \tag{112}$$

the Newton-Raphson method being the canonical example. Assuming dead loads, the submatrices can be written explicitly as

$$\begin{aligned}\{K_{xx}\}_{aibk} &= \left(\frac{\partial^2\mathcal{I}^{\text{eff}}_n(\mathbf{x}_{n+1},\boldsymbol{\phi}_{n+1})}{\partial\mathbf{x}^2_{n+1}}\right)_{aibk} = \int_{B_0}\left(W^{\text{eff}}_{n\,,\boldsymbol{F}_{n+1}\boldsymbol{F}_{n+1}}\right)_{iJkL}N_{a,J}N_{b,L}\,\mathrm{d}V_0\,,\\ \{K_{x\phi}\}_{aib} &= \left(\frac{\partial^2\mathcal{I}^{\text{eff}}_n(\mathbf{x}_{n+1},\boldsymbol{\phi}_{n+1})}{\partial\mathbf{x}_{n+1}\partial\boldsymbol{\phi}_{n+1}}\right)_{aib} = \int_{B_0}\left(W^{\text{eff}}_{n\,,\boldsymbol{F}_{n+1}\phi_{n+1}}\right)_{iJ}N_{a,J}\mathcal{N}_b\,\mathrm{d}V_0\,,\\ \{K_{\phi\phi}\}_{ab} &= \left(\frac{\partial^2\mathcal{I}^{\text{eff}}_n(\mathbf{x}_{n+1},\boldsymbol{\phi}_{n+1})}{\partial\boldsymbol{\phi}^2_{n+1}}\right)_{ab} = \int_{B_0}\left[W^{\text{eff}}_{n\,,\phi_{n+1}\phi_{n+1}}\mathcal{N}_a\mathcal{N}_b + \left(W^{\text{eff}}_{n\,,\boldsymbol{\nabla}\phi_{n+1}\boldsymbol{\nabla}\phi_{n+1}}\right)_{IJ}\mathcal{N}_{a,I}\mathcal{N}_{b,J}\right]\mathrm{d}V_0\,.\end{aligned} \tag{113}$$

Due to the variational structure of the problem, the constitutive tangents $D^2W^{\text{eff}}_n$ and hence the Hessian matrix $D^2\mathcal{I}^{\text{eff}}_n$ are guaranteed to be symmetric, which explains why we have written $\mathbf{K}^T_{x\phi}$ instead of $\mathbf{K}_{\phi x}$ in the lower left block. This also leads one to conclude that $\mathbf{K}_{xx}$ and $\mathbf{K}_{\phi\phi}$ are also each symmetric matrices. In passing, we note that symmetry can be used to reduce storage overhead.

In the implementation, the integrals are carried out in the standard finite element fashion: quadrature is performed on an element-by-element basis, and element contributions to the gradient and Hessian are assembled into the correct places in the global arrays.

6 Solver

We have noted several benefits of casting the problem in minimization form. The solution procedure is where this approach begins to pay real dividends. As an example, we describe one strategy created with a prototype implementation of the model in Matlab and the Optimization Toolbox.

At the start, we make the choice to enforce the irreversibility constraint on the phase field *at the nodes*. This is an approximation, as point-wise violations of the constraint can occur within elements if the shape functions employed are not positive.[5] However, any point-wise violations are expected to be small, and since they are due to interpolation error, one expects such violations to diminish with mesh refinement. The benefit of this choice is flexibility: by delegating the irreversibility constraint to the solver, one makes no commitment to a particular enforcement strategy at the level of the finite element assembly. The implementation is responsible only for providing the gradient vector (i.e., the residual nodal forces) and the Hessian matrix (stiffness matrix) as given previously in Equations (111) and (113) in Section 5.2. For the actual nodal solution, there are a wealth of constrained optimization methods to choose from in mathematical optimization software libraries, allowing one to explore possibilities and tailor the choice of solution algorithm to the problem at hand.

In our prototype, we apply a Newton-Trust Region method with bound constraints. In Matlab parlance, this is the "fmincon" solver with the "trust-region-reflective" option (here "reflective" refers to the strategy for handling bound constraints).[6] We have elected to employ a monolithic structure, solving for both the phase field and the displacements simultaneously. The unknowns are taken to be the increment in the nodal unknowns over the time step, i.e.

$$\mathbf{U} = \begin{bmatrix} \mathbf{x}_{n+1} - \mathbf{x}_n \\ \boldsymbol{\phi}_{n+1} - \boldsymbol{\phi}_n, \end{bmatrix}.$$

At iteration k, the trust region method provides correction vector $\Delta\mathbf{U}^{(k)}$, such that

$$\mathbf{U}^{k+1} = \mathbf{U}^k + \Delta\mathbf{U}^k$$

(Here and in the following, we identify the trust region iteration number of nodal arrays with a superscript). If the updated solution is rejected by the trust region algorithm, the iteration is repeated with a smaller trust region radius. If the solution is accepted, we test for convergence using an energy norm measure (see (Bathe, 2014, Chapter 8.4) and Bathe and Cimento (1980)):

$$-D\mathcal{I}_n^{(k-1)^T}\Delta\mathbf{U}^{(k)} \leq \epsilon_E \left(-D\mathcal{I}_n^{(0)^T}\Delta\mathbf{U}^{(1)}\right)$$

where ϵ_E is the tolerance. We typically use the value of $\epsilon_E = 10^{-9}$. Convergence is typically observed in a small number of nonlinear iterations, say 5–10. If convergence is not reached in an acceptable number of nonlinear iterations, the load increment is abandoned and tried again with a smaller time step. The energy norm measure is motivated by two points: first, it puts the the displacement degrees of freedom (dimensions of length) and the phase (dimensionless) on an equal dimensional footing without an arbitrary weighting factor. Second, phase degrees of freedom with active irreversibility constraints are naturally filtered out, as their correction term in $\Delta\mathbf{U}$ will be zero.

The linear solves at each iteration are accomplished with a direct Cholesky solver for small problems, and with a conjugate gradient method for large problems. The conjugate gradient solver is preconditioned with the default Matlab Jacobi-type method; more efficient choices can surely be brought to bear, if necessary. Note that symmetry of the Hessian matrix, which is required for good performance of the conjugate gradient method, is guaranteed by the variational structure.

The above method is in contrast to the prevailing solution strategy in the literature for phase field fracture models, which adopts a staggered approach. Each time step is split into separate subproblems for the displacement update and phase field update, with possible iterations between the subproblems until both fields are converged. We have not yet performed detailed performance investigations of the

[5] For example, standard Lagrange polynomial basis functions of degree greater than one are not positive.

[6] Similar options can be found in high performance, large-scale optimization packages, such as the BNTR solver in the Petsc/TAO library Balay et al. (2019). The Rapid Optimization Library (ROL) in the Trilinos package Kouri and Ridzal (2014) also offers a similar option.

above method against the conventional phase field fracture solution technique. However, it is reasonable to hope for at least two advantages: first, the monolithic structure might converge faster in problems where the displacement and phase fields are strongly coupled, such as in cracks that are nearly unstable; second, minimization solvers can more readily guard against accepting states that are saddle points and not local minimizers. Alternate minimization techniques are susceptible to this problem without additional precautions.

Remark 6.1. There is an important restriction to observe when using this solution algorithm: elements for which the consistent nodal forces for a spatially uniform load are *zero* or *negative* at any nodes must be avoided. Otherwise, the nodal enforcement strategy of the irreversibility constraint becomes degenerate. A notable example is furnished by quadratic simplex elements with the standard Lagrange polynomial basis, having null forces at the vertex nodes under uniform loads.

In practice, we use the quadratic mixed elements described in the appendix to avoid locking, which have the additional benefit of strictly positive consistent nodal forces under uniform load. The degeneracy problem is thus avoided. □

Appendix

A Volumetric locking

It is well known that volumetric locking afflicts low order elements in problems with significant plastic deformation. In this section we describe modifications to the numerical implementation in order to remedy this difficulty. An important concern is that the variational structure of the framework not be destroyed by the modifications. To this end, we extend the mixed variational principle approach of Simo et al. (1985) to the phase field system. The original functional in primal form is augmented to a Hu-Washizu style functional, with additional discrete fields for the Jacobian and the pressure:

$$\begin{aligned}\mathcal{J}_n(\boldsymbol{\chi}_{n+1}, \phi_{n+1}, \boldsymbol{N}^p_{n+1}, \bar{\varepsilon}^p_{n+1}, p, \Theta) = &\int_{B_0} W_n \left(\left(\frac{\Theta}{J_{n+1}} \right)^{1/d} \boldsymbol{\nabla}\boldsymbol{\chi}_{n+1}, \phi_{n+1}, \boldsymbol{\nabla}\phi_{n+1}, \bar{\varepsilon}^p_{n+1}, \boldsymbol{N}^p_{n+1} \right) \mathrm{d}V_0 \\ &+ \int_{B_0} p\,(J_{n+1} - \Theta)\,\mathrm{d}V_0 - L(\boldsymbol{\chi}_{n+1} - \boldsymbol{\chi}_n, \phi_{n+1} - \phi_n),\end{aligned} \tag{114}$$

where $J_{n+1} = \det \boldsymbol{\nabla}\boldsymbol{\chi}_{n+1}$ in the point-wise sense. The symbol d is the spatial dimension, which is 2 for plane strain or 3 for three-dimensional problems. The pressure and Jacobian fields are drawn from identical function spaces. Thus we write

$$\Theta(\boldsymbol{X}) = \sum_{a=1}^{n_p} L^a(\boldsymbol{X})\Theta^a \qquad p(\boldsymbol{X}) = \sum_{a=1}^{n_p} L^a(\boldsymbol{X}) p^a$$

where the L^a are the shape functions, and n_p is the number of nodes for the pressures and Jacobians. As there are no derivatives of these fields in the objective functional, we are at liberty to take discontinuous basis functions that each have support on only one element. This can be exploited to statically condense these fields out at the element level.

The full mixed functional (114) is notationally cumbersome. Fortunately, it is not necessary to deal with the entire functional at once. As before, the optimization may be logically split into several parts, each corresponding to a different phase of the finite element assembly process. Let

$$\bar{\boldsymbol{F}} = \left(\frac{\Theta}{J_{n+1}} \right)^{\frac{1}{d}} \boldsymbol{F}_{n+1}$$

be the modified deformation gradient appearing in (114). As in the primal method, optimization of the potential with respect to the internal variables defines the constitutive update, and provides the potential

for the generalized forces:

$$W_n^{\text{eff}}\left(\bar{\boldsymbol{F}}, \phi_{n+1}, \boldsymbol{\nabla}\phi_{n+1}\right) = \min_{\bar{\varepsilon}^p_{n+1}\boldsymbol{N}^p_{n+1}} W_n\left(\bar{\boldsymbol{F}}, \phi_{n+1}, \boldsymbol{\nabla}\phi_{n+1}, \boldsymbol{N}^p_{n+1}, \bar{\varepsilon}^p_{n+1}\right)$$

So far, the only departure from the primal method is that the value of the deformation gradient passed to the constitutive update is modified. We have not defined how to compute Θ yet; this will be done at the element level in the following.

To continue, we break up the integrals into contributions from each element domain Ω_E:

$$\mathcal{J}_n^E(\boldsymbol{\chi}_{n+1}, \phi_{n+1}, p, \Theta) = \int_{\Omega_E}\left[W_n^{\text{eff}}\left(\left(\frac{\Theta}{J_{n+1}}\right)^{1/d}\boldsymbol{\nabla}\boldsymbol{\chi}_{n+1}, \phi_{n+1}, \boldsymbol{\nabla}\phi_{n+1}\right) + p\left(J_{n+1}-\Theta\right)\right]\mathrm{d}V_0 - L(\Delta\boldsymbol{\chi}, \Delta\phi)\big|_{\Omega_E}.$$

Due to the local support of the pressure and Jacobian basis functions, we can perform the optimization with respect to those fields at the element level, yielding,

$$\mathcal{J}_E^{\text{eff}}(\boldsymbol{\chi}_{n+1}, \phi_{n+1}) = \sup_p \inf_\Theta \mathcal{J}_n^E(\boldsymbol{\chi}_{n+1}, \phi_{n+1}, p, \Theta)$$

which amounts to static condensation. Explicit representations of these operations is provided in the following. Let $\mathbf{p} = \{p^a, a = 1, 2, \dots Q_E\}$ be the array of nodal pressure degrees of freedom on element E, and the corresponding array for Jacobians be $\boldsymbol{\Theta} = \{p^a, a = 1, 2, \dots Q_E\}$. Let $\mathbf{M}$ be the mass matrix of the pressure basis functions, with components given by

$$M^{ab} = \int_{\Omega_E} L^a(\boldsymbol{X})L^b(\boldsymbol{X})\,\mathrm{d}V_0\,,$$

and let $\mathbf{f}_\Theta$ be the array with components

$$f^a_\Theta = \int_{\Omega_E} J_{n+1}L^a\,\mathrm{d}V_0\,.$$

Maximization with respect to p then yields

$$\mathbf{M}\boldsymbol{\Theta} = \mathbf{f}_\Theta,$$

which is solved for the nodal Jacobian values on element E. The Jacobian field is interpolated to the quadrature points to compute $\bar{\boldsymbol{F}}$ for use in the constitutive update.

Once the constitutive update has been performed at all quadrature points on the element, the pressure field is found as follows. Let $\mathbf{f}_p$ be the array with components

$$f^a_p = \int_{\Omega_E}\frac{1}{d\Theta}\,\mathrm{tr}\Big(\boldsymbol{P}_{n+1}\bar{\boldsymbol{F}}^T\Big)L^a\,\mathrm{d}V_0\,.$$

Then, the minimization condition for Θ yields

$$\mathbf{M}\mathbf{p} = \mathbf{f}_p,$$

which is solved for the pressure degrees of freedom on element E.

At this point, the global functional is assembled from the element contributions as

$$\mathcal{J}_n^{\text{eff}}(\boldsymbol{\chi}_{n+1}, \phi_{n+1}) = \sum_E \mathcal{J}_E^{\text{eff}}(\boldsymbol{\chi}_{n+1}, \phi_{n+1}).$$

As before, the outer problem remains in the form

$$\inf_{\boldsymbol{\chi}_{n+1}\phi_{n+1}} \mathcal{J}_n^{\text{eff}}(\boldsymbol{\chi}_{n+1}, \phi_{n+1}),$$

and thus the global solution method for the deformation and the phase field need not be aware of the mixed method.

Now we provide information on the computation of the gradient and Hessian of the mixed functional. The contribution to the objective function gradient from a generic element E is

$$D\mathcal{J}_E^{\text{eff}} = \begin{bmatrix} \mathbf{r}_x \\ \mathbf{r}_\phi \end{bmatrix},$$

wherein $\mathbf{r}_x$ is now

$$(r_x)_{ai} = \int_{\Omega_E} \bar{P}_{iJ} \left[\frac{\Theta}{J}\right]^{\frac{1}{d}} N^a_{,J} \,\mathrm{d}V_0 - (f_x^{\text{ext}})_{ai}|_{\Omega_E}.$$

The above makes use of the modified Piola stress

$$\bar{\boldsymbol{P}} = \boldsymbol{P} - \frac{1}{d}\operatorname{tr}\Big(\boldsymbol{P}\bar{\boldsymbol{F}}^T\Big)\bar{\boldsymbol{F}}^{-T} + Jp\bar{\boldsymbol{F}}^{-T}.$$

The expression for $\mathbf{r}_\phi$ remains the same as the primal method equation (111)b (integrated over the single element domain Ω_E).

The Hessian matrix contribution for each element is given by a static condensation procedure. First, we define the matrix

$$D^2\mathcal{J}_E = \begin{bmatrix} \mathbf{k} & \mathbf{B} \\ \mathbf{B}^T & \mathbf{D} \end{bmatrix}$$

in which the submatrices are

$$\mathbf{k} = \begin{bmatrix} \mathbf{k}_{xx} & \mathbf{k}_{x\phi} \\ \mathbf{k}_{x\phi}^T & \mathbf{k}_{\phi\phi} \end{bmatrix} \qquad \mathbf{B} = \begin{bmatrix} \mathbf{k}_{x\Theta} & \mathbf{k}_{xp} \\ \mathbf{k}_{\phi\Theta}^T & \mathbf{k}_{\phi p} \end{bmatrix} \qquad \mathbf{D} = \begin{bmatrix} \mathbf{k}_{\Theta\Theta} & \mathbf{k}_{\Theta p} \\ \mathbf{k}^{\Theta p} & \mathbf{0} \end{bmatrix} \tag{115}$$

In writing $\mathbf{D}$ above, we have made use of the fact $\mathbf{k}_{pp} = \mathbf{0}$. Since we eliminate the p and Θ fields at the element level, the Hessian matrix can be reduced to primal form by the Schur complement of (115):

$$D^2\mathcal{J}_E^{\text{eff}} = \mathbf{k} - \mathbf{B}\mathbf{D}^{-1}\mathbf{B}^T$$

The inverse matrix $\mathbf{D}^{-1}$ can be written in the form

$$\mathbf{D}^{-1} = \begin{bmatrix} \mathbf{0} & \mathbf{k}_{\Theta p}^{-T} \\ \mathbf{k}_{\Theta p}^{-1} & -\mathbf{k}_{\Theta p}^T \mathbf{k}_{\Theta\Theta}^{-1} \mathbf{k}_{\Theta p} \end{bmatrix}.$$

Thanks to the fact that the basis functions for p and Θ are the same, the submatrix $\mathbf{k}_{\Theta p}$ is square and invertible.

We provide explicit representations of the submatrices used to compute the Hessian:

$$\mathbf{k}_{\Theta p} = -\mathbf{M}$$

$$\mathbf{k}_{pp} = \mathbf{0}$$

$$(k_{\Theta\Theta})_{ab} = \int_{\Omega_E} \left(\frac{1-d}{d^2\Theta^2}\operatorname{tr}\Big(\boldsymbol{P}\bar{\boldsymbol{F}}^T\Big) + \frac{1}{d^2\Theta^2}(W_n^{\text{eff}}{}_{,\boldsymbol{FF}})_{iJkL}\bar{F}_{iJ}\bar{F}_{kL}\right) L^a L^b \,\mathrm{d}V_0$$

$$(k_{xp})_{aib} = \int_{\Omega_E} J\bar{F}^{-1}_{Ji}\left(\frac{\Theta}{J}\right)^{1/d} N^a_{,J} L^b \,\mathrm{d}V_0$$

$$(k_{x\Theta})_{bkc} = \int_{\Omega_E} \left(\frac{1}{d\Theta}(W_n^{\text{eff}}{}_{,\boldsymbol{FF}})_{iJkL}\bar{F}_{iJ} - \frac{1}{d^2\Theta}(W_n^{\text{eff}}{}_{,\boldsymbol{FF}})_{iJmN}\bar{F}_{iJ}\bar{F}_{mN}\bar{F}^{-1}_{Lk} + P_{kL} - \frac{1}{d}\operatorname{tr}\Big(\boldsymbol{P}\bar{\boldsymbol{F}}^T\Big)\bar{F}^{-1}_{Lk}\right)\left(\frac{\Theta}{J}\right)^{1/d} N^b_{,L} L^c \,\mathrm{d}V_0$$

$$\mathbf{k}_{\phi p} = \mathbf{0}$$

The matrix $\mathbf{k}_{\phi\phi}$ is unchanged from the primal version given in (113).

$$(k_{x\phi})_{aib} = \int_{\Omega_E} (W_n^{\text{eff}}{}_{,\boldsymbol{F}\phi})_{kL} \left(\delta_{ik}\delta_{JL} - \frac{1}{d}\bar{F}_{kL}\bar{F}^{-1}_{Ji}\right)\left(\frac{\Theta}{J}\right)^{1/d} N^a_{,J}\mathcal{N}^b \,\mathrm{d}V_0$$

$$(k_{\phi\Theta})_{ab} = \int_{\Omega_E} \frac{1}{d\Theta}(W_n^{\text{eff}}{}_{,\boldsymbol{F}\phi})_{iJ}\bar{F}_{iJ}\mathcal{N}^a L^b \,\mathrm{d}V_0$$

$$\begin{aligned}(k_{xx})_{aibk} = \int_{\Omega_E} \Bigg\{ & (D^2 W_n^{\text{eff}}{}_{,\boldsymbol{FF}})_{iJkL} N^a_{,J} N^b_{,L} - \frac{1}{d}(D^2 W_n^{\text{eff}}{}_{,\boldsymbol{FF}})_{iJmN}\bar{F}_{mN}\bar{F}^{-1}_{Lk} - \frac{1}{d}(D^2 W_n^{\text{eff}}{}_{,\boldsymbol{FF}})_{mNkL}\bar{F}_{mN}\bar{F}^{-1}_{Ji} \\ & + \frac{1}{d^2}(D^2 W_n^{\text{eff}}{}_{,\boldsymbol{FF}})_{mNpQ}\bar{F}_{mN}\bar{F}_{pQ}\bar{F}^{-1}_{Ji}\bar{F}^{-1}_{Lk} - \frac{1}{d}\bar{P}_{kL}\bar{F}^{-1}_{Lk} - \frac{1}{d}\bar{P}_{iJ}\bar{F}^{-1}_{Ji} \\ & + \frac{1}{d^2}\left(Jp - \mathrm{tr}\left(\boldsymbol{P}\bar{\boldsymbol{F}}^T\right)\right)\bar{F}^{-1}_{Ji}\bar{F}^{-1}_{Lk} + \left(1+\frac{1}{d}\right)Jp\bar{F}^{-1}_{Ji}\bar{F}^{-1}_{Lk}\Bigg\}\left[\left(\frac{\Theta}{J}\right)^{1/d} N^a_{,J}\right]\left[\left(\frac{\Theta}{J}\right)^{1/d} N^b_{,L}\right]\mathrm{d}V_0 \end{aligned} \quad (116)$$

A.1 Function spaces and bases for mixed method

We use a set of function spaces that are known in linear problems to satisfy the LBB conditions, to satisfy the ellipticity condition, and to be optimally accurate. In particular, we adopt the elements of Crouzeix and Raviart (1975). These are simplicial elements, where the pressure and Jacobian fields on each element are taken to be $P_1(E)$, the space of polynomials of degree 1. Recall that no interelement continuity is enforced for these fields. The displacement field is taken to be $P_2^+(B_0) \in H^1(B_0)$, which is the space of functions of polynomials of degree less than or equal to 2, enriched with the lowest degree polynomial bubble function on each element. In $2D$, the bubble function is the one from the cubic triangle element $P_3(E)$. In $3D$, the bubble function is from the quartic tetrahedral element $P_4(E)$. For the sake of simplicity, we take the phase field interpolation identical to the displacement interpolation. The basis functions are shown schematically in Figure 1.

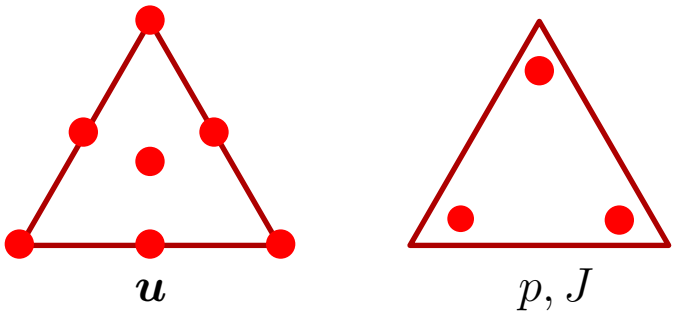

Figure 1: Mixed interpolation.

References

Balay, S., Abhyankar, S., Adams, M.F., Brown, J., Brune, P., Buschelman, K., Dalcin, L., Dener, A., Eijkhout, V., Gropp, W.D., Karpeyev, D., Kaushik, D., Knepley, M.G., May, D.A., McInnes, L.C., Mills, R.T., Munson, T., Rupp, K., Sanan, P., Smith, B.F., Zampini, S., Zhang, H., and Zhang, H., 2019. PETSc Web page. `https://www.mcs.anl.gov/petsc`.

Bathe, K.J., 2014. Finite element procedures. Prentice-Hall, Englewood Cliffs, N.J, 2nd edition. ISBN 978-0-9790049-5-7.

Bathe, K.J. and Cimento, A.P., 1980. Some practical procedures for the solution of nonlinear finite element equations. *Computer Methods in Applied Mechanics and Engineering* 22, 59–85.

Bourdin, B., Francfort, G., and Marigo, J.J., 2000. Numerical experiments in revisited brittle fracture. *Journal of the Mechanics and Physics of Solids* 48(4), 797–826. ISSN 0022-5096. doi: 10.1016/S0022-5096(99)00028-9.

Crouzeix, M. and Raviart, P.A., 1975. Conforming and nonconforming finite element methods for solving the stationary Stokes equations I. *Revue Française d'Automatique Informatique Recherche Opérationnelle Mathématique* 7, 33–75.

Cuvilliez, S., Feyel, F., Lorentz, E., and Michel-Ponnelle, S., 2012. A finite element approach coupling a continuous gradient damage model and a cohesive zone model within the framework of quasi-brittle failure. *Computer Methods in Applied Mechanics and Engineering* 237-240, 244–259. ISSN 00457825. doi:10.1016/j.cma.2012.04.019.

Gurtin, M.E., 2002. A gradient theory of single-crystal plasticity that accounts for geometrically necessary dislocations. *Journal of the Mechanics and Physics of Solids* 50, 5–32. doi:10.1016/S0022-5096(01) 00104-1.

Gurtin, M.E., Fried, E., and Anand, L., 2010. The Mechanics and Thermodynamics of Continua. Cambridge University Press, New York, NY. ISBN 978-0-521-40598-0.

Kouri, D. and Ridzal, D., 2014. Rapid Optimization Library. Technical Report SAND2014-19572 C, Sandia National Laboratories.

Lorentz, E., Cuvilliez, S., and Kazymyrenko, K., 2011. Convergence of a gradient damage model toward a cohesive zone model. *Comptes Rendus Mécanique* 339(1), 20–26. ISSN 16310721. doi:10.1016/j.crme. 2010.10.010.

Lorentz, E., Cuvilliez, S., and Kazymyrenko, K., 2012. Modelling large crack propagation: from gradient damage to cohesive zone models. *International Journal of Fracture* 178(1), 85–95. ISSN 1573-2673. doi:10.1007/s10704-012-9746-7.

Ortiz, M. and Stainier, L., 1999. The variational formulation of viscoplastic constitutive updates. *Computer Methods in Applied Mechanics and Engineering* 171(3), 419–444. ISSN 0045-7825. doi: 10.1016/S0045-7825(98)00219-9.

Pham, K., Amor, H., Marigo, J.J., and Maurini, C., 2011. Gradient Damage Models and Their Use to Approximate Brittle Fracture. *International Journal of Damage Mechanics* 20(4), 618–652. ISSN 1056-7895, 1530-7921. doi:10.1177/1056789510386852.

Radovitzky, R. and Ortiz, M., 1999. Error estimation and adaptive meshing in strongly nonlinear dynamic problems. *Computer Methods in Applied Mechanics and Engineering* 172(1-4), 203–240. ISSN 00457825. doi:10.1016/S0045-7825(98)00230-8.

Sansour, C., 2001. On the dual variable of the logarithmic strain tensor, the dual variable of the Cauchy stress tensor, and related issues. *International Journal of Solids and Structures* 38(50), 9221–9232. ISSN 0020-7683. doi:10.1016/S0020-7683(01)00073-7.

Simo, J., Taylor, R., and Pister, K., 1985. Variational and projection methods for the volume constraint in finite deformation elasto-plasticity. *Computer Methods in Applied Mechanics and Engineering* 51(1-3), 177–208. ISSN 00457825. doi:10.1016/0045-7825(85)90033-7.

Weber, G. and Anand, L., 1990. Finite deformation constitutive equations and a time integration procedure for isotropic, hyperelastic-viscoplastic solids. *Computer Methods in Applied Mechanics and Engineering* 79(2), 173–202. ISSN 0045-7825. doi:10.1016/0045-7825(90)90131-5.